

AD-A031 426

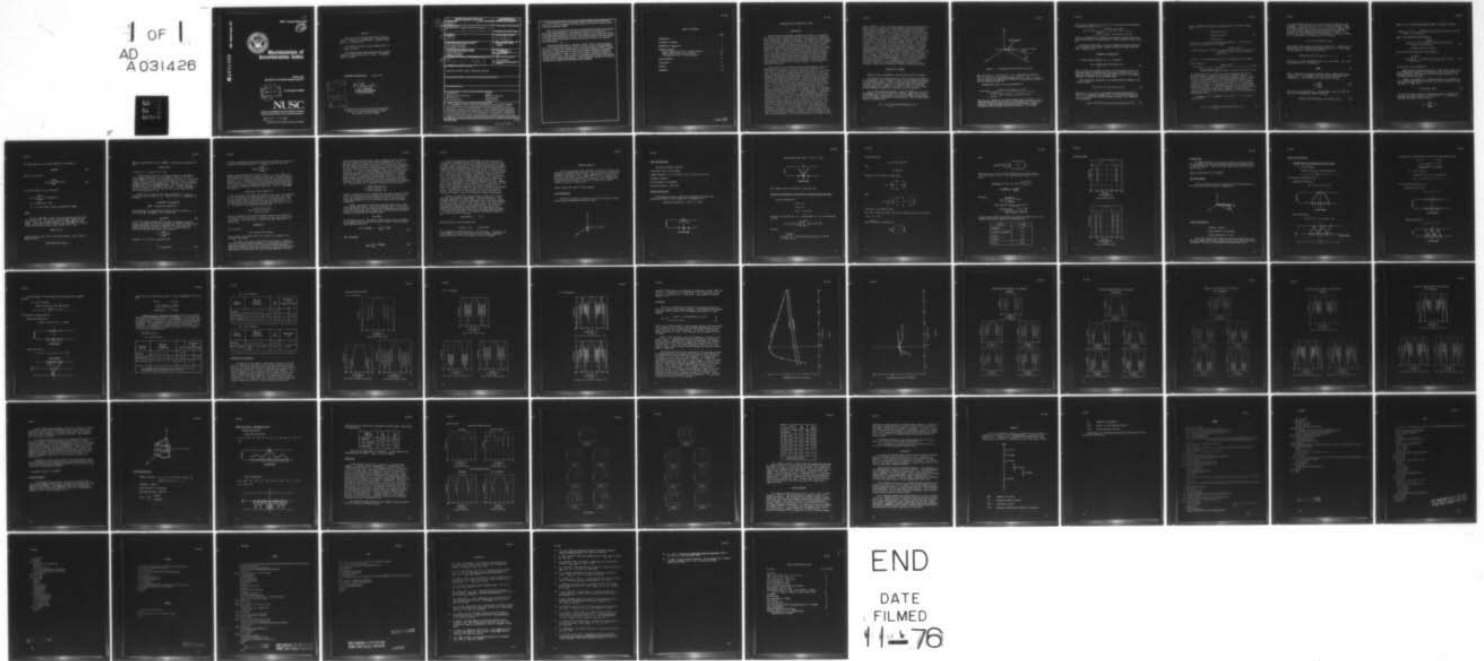
NAVAL UNDERWATER SYSTEMS CENTER NEW LONDON CONN NEW --ETC F/G 17/1
MAXIMIZATION OF REVERBERATION INDEX.(U)
OCT 76 D LEE

UNCLASSIFIED

NUSC-TR-5375

NL

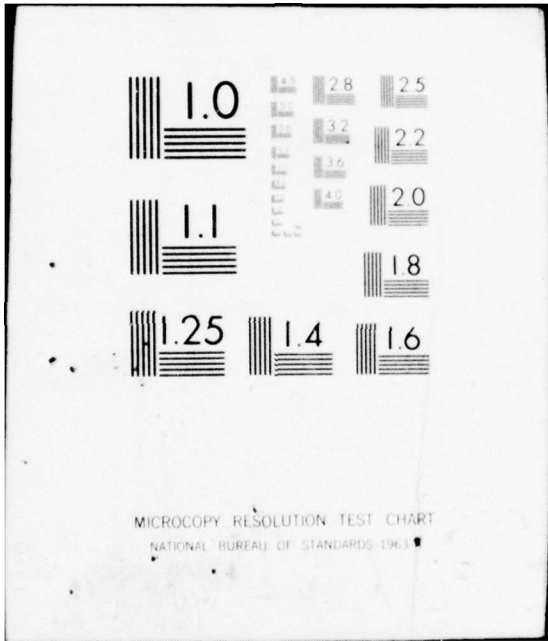
1 OF 1
AD
A031426



END

DATE
FILMED

11-76



NUSC Technical Report 5375

AD A 031 426

NUSC Technical Report 5375

FG

12



Maximization of Reverberation Index

Ding Lee
Systems Analysis Department

DDC
RECEIVED
NOV 2 1976
REGULATED
B

2 October 1976

NUSC

NAVAL UNDERWATER SYSTEMS CENTER
Newport, Rhode Island • New London, Connecticut

Copy available to DDC does not permit fully legible reproduction

Approved for public release; distribution unlimited.

PREFACE

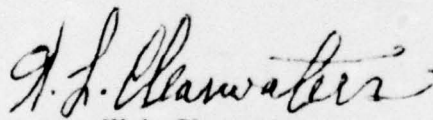
This research was conducted under NUSC Project No. 301809, "Conformal Array Applications," Principal Investigator, T. G. Bell (Code 22).

The Technical Reviewer for this report was Dr. N. L. Owsley (Code 315).

The author gratefully acknowledges the many valuable discussions which he had with T. G. Bell, J. J. Hanrahan, and W. F. Wardle.

REVIEWED AND APPROVED: 2 October 1976

ACCESSION for	
NTIS	White Section <input checked="" type="checkbox"/>
DDC	Buff Section <input type="checkbox"/>
UNANNOUNCED	<input type="checkbox"/>
JUSTIFICATION	
BY	
DISTRIBUTION/AVAILABILITY CODES	
Dist.	AVAIL. and/or SPECIAL
A	



W. L. Clearwaters
Associate Technical Director
for Plans and Analysis

The author of this report is located at the New London Laboratory, Naval Underwater Systems Center, New London, Connecticut 06320.

in that the omnidirectional ambient noise limited condition can be considered a specific case of the more general directional ambient noise limited condition and the reverberation limited condition.

Much of the existing theory that has been developed has been directed at specific cases, thus leaving unfinished a comprehensive treatment of the general case. A concomitant existing problem involves the determination of the computational complexity involved in the mathematical solution to the described problems since this complexity strongly influences the degree to which computational methods can be applied to practical problems.

The purpose of this paper is, therefore, twofold. First, to solve the general case, the RI maximization problem; second, to provide insofar as possible efficient numerical procedures for implementation of the general solution in various practical applications. These objectives are achieved by detailed mathematical formulation based on matrix theory, which, as will be shown, yields a complete procedure for solving the general case. This procedure is sufficiently generalized so that the maximization of DI is automatically included. Several illustrative examples are included to demonstrate the validity and effectiveness of this technique.

TABLE OF CONTENTS

	Page
INTRODUCTION	1
STATEMENT OF PROBLEM	2
MATHEMATICAL FORMULATION	4
NUMERICAL RESULTS	13
Equally Spaced Line Array of Three Elements.	13
Equally Spaced Array of Six Elements	19
A Cylindrical Array of Fifteen Elements.	36
FUTURE RESEARCH	43
CONCLUSIONS	44
APPENDIX	A-1
REFERENCES	R-1

MAXIMIZATION OF REVERBERATION INDEX

INTRODUCTION

Within the past two decades, problems with respect to maximizing the directive gain of antenna arrays have been extensively studied and some solutions have already been produced. Concerning the optimization, Uzkov¹ presented an approach to the problem of optimum directive antennae design and obtained some important results; Tai² discussed the optimum directivity of uniformly spaced broadside arrays of dipoles; Butler³ considered the optimization problem of nonuniformly spaced arrays; Ma,⁴ Cheng, and Tseng^{5,6} presented an approach to optimize arbitrary antenna arrays; Lo, Lee, and Lee⁷ optimized directivity and signal-to-noise ratio of an arbitrary array; Gilbert and Morgan⁸ discussed optimum design of directive antenna array subject to random variation; Mermoz⁹ showed that matched filtering techniques applied to particular conditions of crosscorrelation created at the antenna by omnidirectional noise produce the optimization of the directivity; contributions have also been made by others such as Block,¹⁰ Riblet,¹¹ Chu,¹² Yaru,¹³ Wilmotte¹⁴ and others.

In the sonar area, investigations have been conducted related to maximizing the array gain of an array dominated by ambient noise. Pritchard^{15,16} discussed the maximum directivity index (DI) of a linear array; Farran and Hill¹⁷ studied wide-band directivity of receiving arrays and applied Lagrange multipliers to maximize directivity index; Edleblute¹⁸ introduced an optimum-signal-detection theory and used the signal-to-noise criteria to maximize DI; Cox¹⁹ discussed the optimization problems taking sensitivity into consideration; optimum signal processing was discussed by Bryn,²⁰ Nuttall,²¹ Owsley,²² Lewis,²³ and others. These studies have developed mathematical solutions for the optimization of DI with significant promise of practical applications. A related important optimization problem arises when the background interference is nonisotropic, for example, when it is reverberation related or when ambient noise is itself nonisotropic. Under such a condition, the general solution, i.e., the reverberation index (RI) optimization is required. The RI optimization problem was never considered previously. Adherence to the solution for the general case throughout all phases from the initial problem formulation to final modeling technique allows all aspects of an array's directivity to be investigated using essentially the same mathematical procedure. In order to encompass the already existing theory, some adaptation was necessary within the work of the general case in the formulation of mathematical technique. As noted earlier, an important part of the development of these techniques is related to the investigation of the degree of computational complexity necessary for the practical utilization of these techniques. In view of the preceding, the purpose of this

paper is twofold. First, to solve, in general, the RI maximization problem; second, to achieve the complete feasible numerical treatment to various practical applications. The entire problem is mathematically formulated and is handled by means of the treatment used for eigenvalue (Gantmacher²⁴) problems. This technique will express the RI as a ratio of two quadratic forms that determine an optimum set of amplitude and phase excitations to yield the maximum RI. This procedure is developed with sufficient generality so that the maximization of DI is included automatically. This paper states the problem, presents a section of theoretical formulation, and includes a section of three illustrative examples. A later section also discusses remaining research problems. Some conclusions are drawn from the theoretical viewpoint. The basic computer programs that have been developed to perform the necessary computations on UNIVAC 1108 computer are included in the appendix. The calculation of beam patterns, RI, and DI is carried out by the GBEAM (Lee²⁵) program. Implementation of this technique ideally requires a complete automation of computer programs. Such a package is already under our consideration and development, but is not yet available at this reporting period. It is believed that once this model is developed, research can proceed and meaningful solutions can be obtained to address more complicated, presently unanswered problems.

STATEMENT OF PROBLEM

Before we state the problem, a few definitions have to be made.

We consider the coordinate system for array structure according to the configuration shown in figure 1, where θ is the azimuthal deviation in the horizontal plane, ϕ is the vertical deviation from a horizontal reference, and $0 \leq \theta \leq 2\pi$, $-\pi/2 \leq \phi \leq \pi/2$. A reference plane for measuring relative phase at any element of the array is chosen to be that plane passing through the origin that is parallel to all wavefronts.

Let R_j be the amplitude response at the j^{th} element, $d_j(\theta, \phi)$ be the distance from the j^{th} element to a reference plane that is taken to be perpendicular to the direction (θ, ϕ) of the incoming acoustic waves, and α_j are unknown coefficients to be determined. Then, the beam output function is defined to be

$$V(\theta, \phi, \alpha_j) = \sum_{j=1}^n \alpha_j R_j \exp[i(2\pi/\lambda)d_j(\theta, \phi)].$$

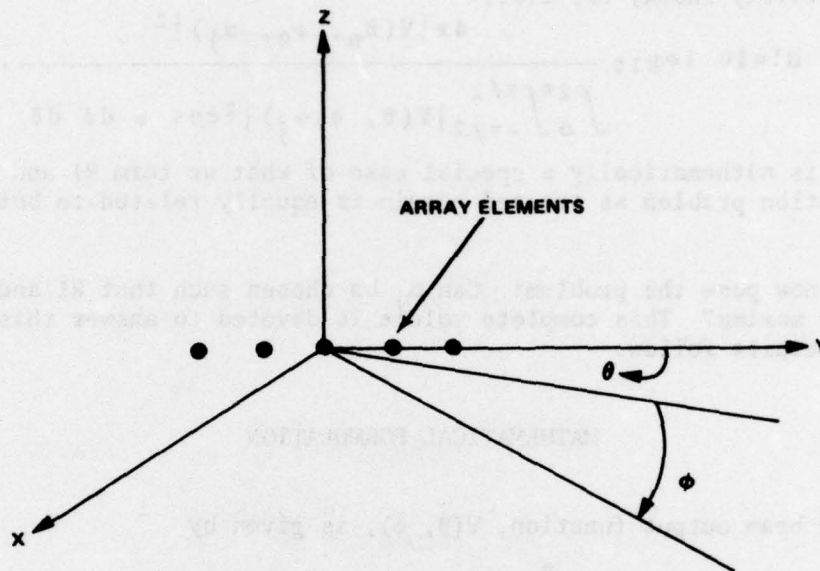


Figure 1. A 3-Dimensional Array Geometry Structure

When $\alpha_j=1$ for all j , the term $V(\theta, \phi, 1)$, conventionally written as $V(\theta, \phi,)$ refers to an unshaded beam output function. $V(\theta, \phi, \alpha_j)$ is used to calculate the beam pattern function, the reverberation index RI, and the directivity index DI.

Reverberation index, RI, can be expressed as

$$RI = 10 \log_{10} \frac{2\pi(\sin b - \sin a) |V(\theta_0, \phi_0, \alpha_j)|^2}{\int_0^{2\pi} \int_a^b \{RV(\theta, \phi)\} |V(\theta, \phi, \alpha_j)|^2 \cos \phi \, d\phi \, d\theta}$$

where (θ_0, ϕ_0) stands for steering direction angles and $RV(\theta, \phi)$ is a reverberation function that is used to characterize the relative reverberation strength of backscattered energy from boundary or volume scatterers over the angular intervals of interest. If we assign

$a=-\pi/2$, $b=\pi/2$, and $RV(\theta, \phi)=1$ for all θ, ϕ , we arrive at the expression of directivity index, DI, i.e.,

$$DI = 10 \log_{10} \frac{4\pi |V(\theta_0, \phi_0, \alpha_j)|^2}{\int_0^{2\pi} \int_{-\pi/2}^{\pi/2} |V(\theta, \phi, \alpha_j)|^2 \cos \phi \, d\phi \, d\theta}$$

Thus DI is mathematically a special case of what we term RI and so the optimization problem as treated herein is equally related to both RI and DI.

We now pose the problem: Can α_j be chosen such that RI and DI are at their maxima? This complete volume is devoted to answer this question. Details follow.

MATHEMATICAL FORMULATION

The beam output function, $V(\theta, \phi)$, is given by

$$V(\theta, \phi) = \sum_{j=1}^n R_j \exp [i(2\pi/\lambda)d_j(\theta, \phi)], \quad (1)$$

where θ defines the azimuthal deviation in the horizontal plane, ϕ defines the vertical deviation from a horizontal reference, R_j is the amplitude response of the j -th element, and $d_j(\theta, \phi)$ is the distance from the j -th element to the reference plane.

For a plane wave excitation, the distance from any element to the reference plane is

$$d_j(\theta, \phi) = x_j \cos \alpha + y_j \cos \beta + z_j \cos \gamma, \quad (2)$$

where $(\cos \alpha, \cos \beta, \cos \gamma)$ are direction cosines which define the direction of propagation perpendicular to the incoming wavefront and (x_j, y_j, z_j) stands for Cartesian element location. For a spherical wave excitation,

$$d_j(\theta, \phi) = r_0 - [(x_j - x_\xi)^2 + (y_j - y_\xi)^2 + (z_j - z_\xi)^2]^{1/2}, \quad (3)$$

where r_0 defines the distance of a point source to the array center, and

$$\begin{aligned}x_{\xi} &= r_0 \cos \phi \sin \theta, \\y_{\xi} &= r_0 \cos \phi \cos \theta, \\z_{\xi} &= -r_0 \sin \phi.\end{aligned}\tag{4}$$

For details, the reader should consult reference 25. The directivity index, DI, is expressed by the formula.

$$DI = 10 \log_{10} \Delta_1 = 10 \log_{10} \frac{|V(\theta_0, \phi_0)|^2}{\frac{1}{4\pi} \int_0^{2\pi} \int_{-\pi/2}^{\pi/2} |V(\theta, \phi)|^2 \cos \phi \, d\phi \, d\theta},\tag{5}$$

(Urick²⁶). The reverberation index, RI, is expressed by the formula,

$$\begin{aligned}RI &= 10 \log_{10} \Delta_2 \\&= 10 \log_{10} \frac{|V(\theta_0, \phi_0)|^2}{\frac{1}{2\pi(\sin b - \sin a)} \int_0^{2\pi} \int_a^b \{RV(\theta, \phi)\} |V(\theta, \phi)|^2 \cos \phi \, d\phi \, d\theta}\end{aligned}\tag{6}$$

The optimization of DI and RI is the same as optimizing Δ_1 and Δ_2 . We shall attempt to optimize RI and DI in a systematic manner. In general terms, we consider the reverberation function, $RV(\theta, \phi)$, which is used to characterize the relative reverberation strength of back-scattered energy from boundary or volume scatterers over the angular intervals of interest. In the event, the $RV(\theta, \phi)$ is a transmitting beam output function, the introduction of amplitude and phase shading coefficients to $RV(\theta, \phi)$ should be of interest for future research, but it is not considered in our present treatment. Our approach is to maximize Δ_2 and we will show that maximization of Δ_2 accommodates the maximization of Δ_1 .

Introduce a set of n elements, $\{\alpha_j\}$, $j=1, 2, \dots, n$, to $V(\theta, \phi)$. Then we obtain

$$V(\theta, \phi, \alpha_j) = \sum_{j=1}^n \alpha_j R_j \exp [i(2\pi/\lambda) d_j(\theta, \phi)].\tag{7}$$

α_j is the j^{th} amplitude excitation called shading coefficients to be determined. If $\alpha_j=1$ for all j , $V(\theta, \phi, 1) = V(\theta, \phi)$, which is simply an unshaded beam output function. If α_j turn out to be complex, they can be put in polar form; the magnitude part gives the amplitude excitation and the argument part gives the phase excitation. To be general, we consider the problem of maximizing Δ_2 . Once this is done, it is a simple matter to maximize Δ_1 by just setting

$$a=-\pi/2, b=\pi/2 \text{ and } RV(\theta, \phi)=1,$$

which implies that formula (6) reduces to formula (5). Without loss of generality, we drop the amplitude responses for $V(\theta, \phi, j)$ for formulation simplicity. Define a vector \mathbf{E} to be

$$\mathbf{E}=\{\exp[-i(2\pi/\lambda)D_j(\theta_0, \phi_0)]\}, j=1, 2, \dots, n, \quad (8)$$

where $D_j(\theta_0, \phi_0)$ are steering-direction, (θ_0, ϕ_0) , delays. Let: \mathbf{A} be a square matrix that is obtained by

$$\mathbf{A}=\mathbf{E}\mathbf{E}^*, \quad (9)$$

where $*$ indicates the conjugate transpose, \mathbf{B} be a square matrix whose elements are to be determined, and α be a vector consisting of the components α_j . Δ_2 of formula (6) can be put in the form

$$\Delta_2 = \frac{\alpha^* \mathbf{A} \alpha}{\alpha^* \mathbf{B} \alpha} \quad (10)$$

Now our aim is to maximize Δ_2 . Setting $\alpha^* \mathbf{A} \alpha = |V(\theta_0, \phi_0, \alpha_j)|^2$ enables us to determine the elements of $\mathbf{A}=(a_{jk})$,

$$a_{jk}=\exp[i(2\pi/\lambda)(D_j(\theta_0, \phi_0)-D_k(\theta_0, \phi_0))], \quad (11)$$

where (θ_0, ϕ_0) are steering-direction angles. Similarly, setting

$$\alpha^* B \alpha = \frac{1}{2\pi(\sin b - \sin a)} \int_0^{2\pi} \int_a^b \{RV(\theta, \phi)\} |V(\theta, \phi, \alpha_j)|^2 \cos \phi \, d\phi \, d\theta$$

gives the determination of B elements,

$$b_{jk} = \frac{1}{2\pi(\sin b - \sin a)} \int_0^{2\pi} \int_a^b \exp[i(2\pi/\lambda)(d_j - d_k)] \times \{RV(\theta, \phi)\} \cos \phi \, d\phi \, d\theta. \quad (12)$$

For $a = -\pi/2$, $b = \pi/2$, $RV(\theta, \phi) = 1$, (12) reduces to

$$b_{jk} = \frac{1}{4\pi} \int_0^{2\pi} \int_{-\pi/2}^{\pi/2} \exp[i(2\pi/\lambda)(d_j - d_k)] \cos \phi \, d\phi \, d\theta. \quad (12')$$

We shall use (12') to maximize DI.

$\alpha^* B \alpha$ represents reverberation power received by the array; it has to be positive from physical considerations. This implies that B is positive-definite. Therefore Δ_2 can be maximized according to the following optimization theory:

If $A(\alpha, \alpha)$ and $B(\alpha, \alpha)$ are 2 quadratic forms in the variables α_j and if B is positive-definite, then the characteristic equation of the form $A(\alpha, \alpha) - \lambda B(\alpha, \alpha)$ is

$$p(\lambda) = \det(A - \lambda B) = 0. \quad (13)$$

In view of the matrix theory for eigenvalue problems (Gantmacher²⁴), $p(\lambda)$ has real roots λ_j and $\lambda_j \leq \lambda_{j+1}$ for $j=1, 2, \dots, n-1$ and λ_1, λ_n represent the bounds of (10), that is,

$$\lambda_1 \leq \frac{\alpha^* A \alpha}{\alpha^* B \alpha} \leq \lambda_n$$

The right equality of the above expression is attained if

$$\mathbf{A}\mathbf{a} = \lambda_n \mathbf{B}\mathbf{a}. \quad (14)$$

Then, it is seen that

$$\lambda_n = \Delta_2 = \frac{\mathbf{a}^* \mathbf{A} \mathbf{a}}{\mathbf{a}^* \mathbf{B} \mathbf{a}} = \mathbf{E}^* \mathbf{B}^{-1} \mathbf{E} > 0. \quad (15)$$

To justify formula (15) we will prove:

- (a) $\lambda_n = \frac{\mathbf{a}^* \mathbf{A} \mathbf{a}}{\mathbf{a}^* \mathbf{B} \mathbf{a}}$ for "optimum" \mathbf{a} ,
- (b) $\lambda_n = \mathbf{E}^* \mathbf{B}^{-1} \mathbf{E} > 0$, and
- (c) λ_n is the largest nonzero eigenvalue of $(\mathbf{A} - \lambda \mathbf{B})$.

Proof

In view of $\mathbf{A}\mathbf{a} = \lambda_n \mathbf{B}\mathbf{a}$, we shall take inner products of both sides with respect to \mathbf{a}^* . As a result, we obtain $\mathbf{a}^* \mathbf{A} \mathbf{a} = \lambda_n \mathbf{a}^* \mathbf{B} \mathbf{a}$, and (a) results. Next, the conjugate transposition of $\mathbf{A}\mathbf{a} = \lambda_n \mathbf{B}\mathbf{a}$ gives $\mathbf{a}^* \mathbf{A}^* = \lambda_n \mathbf{a}^* \mathbf{B}^*$. Since \mathbf{A} , \mathbf{B} are both Hermitian, then $\mathbf{a}^* \mathbf{A} = \lambda_n \mathbf{a}^* \mathbf{B}$. By virtue of the positive-definite property of \mathbf{B} , the \mathbf{B}^{-1} exists, then

$$\mathbf{a}^* \mathbf{A} \mathbf{B}^{-1} = \mathbf{a}^* \lambda_n.$$

Postmultiply \mathbf{E} on both sides of the above equation, and in view of $\mathbf{E}\mathbf{E}^* = \mathbf{A}$, we obtain

$$(\mathbf{a}^* \mathbf{E}) (\mathbf{E}^* \mathbf{B}^{-1} \mathbf{E}) = (\mathbf{a}^* \mathbf{E}) \lambda_n.$$

α^*E is a nonzero scalar $\rightarrow \lambda_n = E^*B^{-1}E$. The positive-definiteness of $B \rightarrow$

$$\lambda_n = E^*B^{-1}E > 0.$$

(a) and (b) show formula (15) is true.

We just proved that λ_n is a nonzero eigenvalue of $(A-\lambda_n B)\alpha=0$. Now, we want to show that λ_n is the largest. Since E is an $(n \times 1)$ vector, $EE^*=A$ must be an $(n \times n)$ singular matrix of rank 1. Since every column of A is a constant times E (as in every row), there is only one linearly independent column vector of A . Since B is positive-definite, $(A-\lambda_n B)\alpha=0$ can be solved by $B(B^{-1}A-\lambda_n I)\alpha=0$. A is of rank 1, B^{-1} is positive-definite, and $(B^{-1}A)$ must have rank 1. Therefore, $(A-\lambda_n B)\alpha=0$ has only one nonzero eigenvalue and the rest of the eigenvalues are zero of multiplicity $(n-1)$.

Since $\lambda_n > 0$, λ_n must be the largest eigenvalue. Thus (c) is proved and justifies equation (15). Making use of (b), $\lambda_n = E^*B^{-1}E$, and we obtain

$$\begin{aligned} \lambda_n E &= EE^*B^{-1}E \rightarrow \lambda_n E = AB^{-1}E \rightarrow \\ (AB^{-1} - \lambda_n I)E &= 0 \rightarrow (A - \lambda_n B)B^{-1}E = 0. \end{aligned}$$

Therefore $B^{-1}E$ is the eigenvector associated with the nonzero λ_n . In view of $A\alpha = \lambda_n B\alpha$, $(A - \lambda_n B)\alpha = 0$, and it follows that

$$\alpha_{opt} = B^{-1}E, \quad (16)$$

which is the required eigenvector and hence the optimum excitation vector. Equations (15) and (16) constitute the complete solution to the optimization problem and these can be applied to any sonar array. It should be noted that once B^{-1} is found, it is a simple matter to calculate RI and DI since formula (15) reduces to

$$\Delta_2 = \frac{\alpha^* A \alpha}{\alpha^* B \alpha} = E^* \alpha.$$

Therefore, RI or DI can be calculated from

$$10 \log_{10}(E^* \alpha). \quad (17)$$

In order to appreciate the physical significance of equations (5) and (6), consider the following situation: For $\alpha \neq \alpha_{opt}$ it must be true that

$$\mathbf{E}^* \mathbf{B}^{-1} \mathbf{E} = \frac{\alpha^* \mathbf{A} \alpha}{\alpha^* \mathbf{B} \alpha} < \lambda n.$$

Suppose we set $\alpha = \mathbf{E} = \{\exp[-i(2\pi/\lambda)D_j]\}^T$, ($j=1, 2, \dots, n$). This is a typical solution to the array steering problem for the situation where the delays D_j are selected to provide an array MRA at selected steering angles (θ_0, ϕ_0) . Although this solution does not generally yield the maximum value of DI, it possesses the more generally encountered character of array directivity computations and so can be used to relate the term in (15) to appropriate physical quantities. That is, since $\mathbf{A} = \mathbf{E} \mathbf{E}^*$, the quantity

$$\alpha^* \mathbf{A} \alpha = (\mathbf{E}^* \mathbf{E}) \cdot (\mathbf{E}^* \mathbf{E}) = (\mathbf{E}^* \mathbf{E})^2 = n^2$$

is just the square of the number of elements in the array. The numerator of (15) is therefore the signal power of the array output when a perfectly coherent signal of unit amplitude is exciting the array. Also for this special type of shading it is clear that signal power is at maximum (assuming that the α_j are normalized such that $|\alpha_j| \leq 1$ for all j). Passing now to the matrix \mathbf{B} we can show that

$$b_{jk} = \frac{\sin [(2\pi/\lambda)(d_j - d_k)]}{(2\pi/\lambda)(d_j - d_k)},$$

which is recognized as the crosscorrelation between array elements in the presence of isotropic noise. Thus \mathbf{B} is the crosscorrelation matrix of the noise. With the choice of α previously made, $\alpha = \mathbf{E} \rightarrow \mathbf{B}^{-1} = \mathbf{I}$ it follows that

$$\alpha^* \mathbf{B} \alpha = \mathbf{E}^* \mathbf{E} = n.$$

Thus (15) gives

$$DI = 10 \log_{10} n^2/n = 10 \log_{10} n,$$

and so yields a well known result for an array of n elements in an isotropic noise field.

The central aim of this investigation that exhibits a departure from the usual array design procedure, is the maximization of the ratio expressed in equation (15) so as to obtain best system performance. Since α must differ from the vector \mathbf{E} , which we shall assign the special notation α_0 for reasons that will shortly become apparent, it can be

seen that signal sensitivity must suffer accordingly because the numerator of (15) will be driven away from its maximum value. It is a desirable objective, however, since the result of optimization of the DI will usually justify the disadvantage of a reduced array sensitivity. One must consider the overall system performance to fully appreciate this point. It may have become apparent to the reader that the term DI as used in this report is more accurately termed array gain since the method when applied is by no means restricted either to an isotropic noise field or to a perfectly coherent signal excitation. In this general usage, we shall define the matrix **A** as the cross-correlation matrix of the signal with elements a_{jk} and the matrix **B** as the cross-correlation of noise (or any interfacing array excitation) with elements b_{jk} . The expression (15) is therefore a maximization of array gain

$$\lambda_n = \frac{\mathbf{a}^* \mathbf{A} \mathbf{a} \sum_j \sum_k \mathbf{a}_j \mathbf{a}_k a_{jk}}{\mathbf{a}^* \mathbf{B} \mathbf{a} \sum_j \sum_k \mathbf{a}_j \mathbf{a}_k b_{jk}}.$$

Clearly, if the array is to be optimized for an actual real-world situation it is necessary to obtain sufficiently accurate estimates of the array crosscorrelations for both signals and noise that accurately depict the performance of the system under study and the environment encountered.

Further consideration of the matrix **B** yield some measure of how nearly optimum the array is, when in the unshaded state. In the case of DI (and also for RI) we see that **B** can be separated into the identity matrix and a matrix \mathbf{B}_1 , whose elements are (for all practical cases of interest) less than unity in absolute value.

$$\mathbf{B} = (\mathbf{I} + \mathbf{B}_1).$$

In some practical cases, the spectral radius of \mathbf{B}_1 is less than unity. This property of \mathbf{B}_1 is sufficient to allow inversion of **B** by a Neumann series expansion, that is,

$$\mathbf{B}^{-1} = \mathbf{I} - \mathbf{B}_1 + \mathbf{B}_1^2 - \dots = \sum_{\ell=0}^{\infty} (-1)^\ell \mathbf{B}_1^\ell. \quad (18)$$

Thus using $\mathbf{E} = \mathbf{a}_0$,

$$\mathbf{a}_{\text{opt}} = \sum_{\ell=0}^{\infty} (-1)^\ell \mathbf{B}_1^\ell \mathbf{a}_0 \quad (19)$$

The series representation of \mathbf{B}^{-1} shows that \mathbf{a}_{opt} can be partitioned into a convergent sequence of component terms. The first term is equal to \mathbf{a}_0 and this part of \mathbf{a}_{opt} as previously indicated is simply the usual array-steering vector. The degree of optimization attainable beyond this base performance depends on the nature of the matrix \mathbf{B}_1 . If $\mathbf{B}_1=0$ no further optimization is possible (as will be shown in example 2 in a later section) and $\mathbf{a}_{\text{opt}}=\mathbf{E}$, (the unshaded array) is already optimum. Conversely, if \mathbf{B}_1 has elements sufficiently removed from zero, there is an opportunity for further optimization. This is illustrated in the next section where a superdirective condition is imposed on a line array with steering to endfire and element spacing $<(\frac{1}{2})\lambda$. This results in a large number of off-diagonal elements in the matrix \mathbf{B} which gives rise to meaningful terms in addition to the initial term. If the array element separation is taken as an interger multiple of $(\frac{1}{2})\lambda$, however, the matrix \mathbf{B}_1 vanishes and the array is optimum in the unshaded state. The argument has shown (at least in the case of perfectly coherent signal) that it is the nature of the noise statistics that dictates the degree to which array shading can improve performance.

Clearly the larger the crosscorrelation between array elements, the better the change for improvement. Viewed in another way, the technique identifies, by purely mathematical means, the array shading required to minimize the noise-power output of the array while influencing the signal-power output to some lesser degree. Only under some very special situations, the series expansion of \mathbf{B}^{-1} can be used effectively for obtaining a sufficiently close approximation of \mathbf{a}_{opt} without undertaking the horrendous task of inverting large matrices as is the case for large arrays. Letting $\mathbf{a}_0=\mathbf{E}$, succeeding estimates of \mathbf{a}_{opt} can be given by the iteration

$$\mathbf{a}_v = \mathbf{a}_0 + \mathbf{B}_1 \mathbf{a}_{v-1} \quad v \geq 1,$$

and the sequence can be continued until

$$\|\mathbf{a}_v - \mathbf{a}_{v-1}\| < \epsilon, \quad \epsilon \text{ arbitrary,}$$

so as to approach sufficiently close to the limit \mathbf{a}_{opt} . In general, due to the number of arithmetic operations involved and the large memory storage requirement, the series expansion is not recommended.

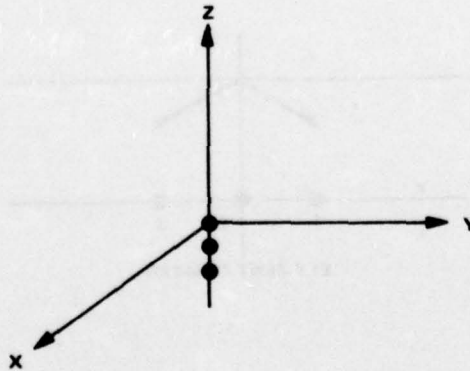
NUMERICAL RESULTS

In the sections below three different arrays that illustrate this technique are described and discussed. The calculations for the first example are performed by hand. Other computations are carried out by the UNIVAC 1108 computer using GBEAM (Lee²⁵) and other programs that have been developed to implement this technique. In all computations, single-precision arithmetic is used and the individual elements' response is absent of consideration.

EQUALLY SPACED LINE ARRAY OF THREE ELEMENTS

Array Description

On the first example, we present an endfire line array of three equally spaced elements placed on the z-axis.



Input Considerations

The input parameters used are:

z-spacing= $\lambda/4$ where λ =wavelength

Element locations: $(0, 0, (-1/2)\lambda)$, $(0, 0, (-1/4)\lambda)$, $(0, 0, 0)$

Frequency = 4900 Hz

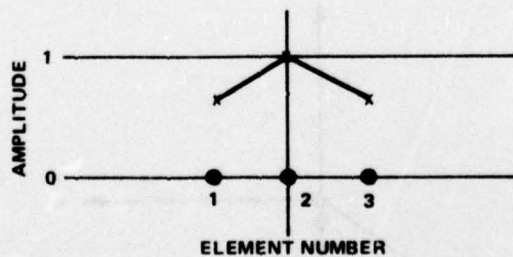
Plane wavefront is considered

Steering direction: $(90^\circ, 90^\circ)$

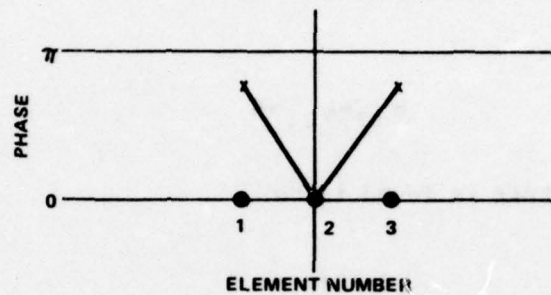
Shading Coefficients

After normalization and separation of amplitude and phase, the shading coefficients of this example are determined to be:

Amplitude Coefficients: $(0.66, 1.0, 0.66)$



Phase Coefficients (rad): (2.85, 0, 2.85)



How to obtain these coefficients is described next.

Analytical and Numerical Calculations of Maximum Directivity Index

From our formulation,

$$\cos \alpha = 0,$$

$$\cos \beta = 0,$$

$$\cos \gamma = -z_j \sin \phi,$$

then $d_j = -z_j \sin \phi$ for $j=1, 2, 3$. Using formula (12') to calculate b_{jk} , we find

$$b_{11} = b_{22} = b_{33} = \frac{1}{4\pi} \int_0^{2\pi} \int_{-\pi/2}^{\pi/2} \cos \phi \, d\phi \, d\theta = 1.$$

For $j \neq k$,

$$b_{jk} = \frac{1}{4\pi} \int_0^{2\pi} \int_{-\pi/2}^{\pi/2} \exp[i(2\pi/\lambda)(d_j - d_k)] \cos \phi \, d\phi \, d\theta.$$

Calculations give

$$b_{12} = b_{21} = b_{23} = b_{32} = 2/\pi$$

and

$$b_{13} = b_{31} = 0.$$

Therefore, the B matrix is found to be

$$B = \begin{pmatrix} 1 & 2/\pi & 0 \\ 2/\pi & 1 & 2/\pi \\ 0 & 2/\pi & 1 \end{pmatrix}$$

and

$$B^{-1} = \frac{1}{8 - \pi^2} \begin{pmatrix} 4 - \pi^2 & 2\pi & -4 \\ 2\pi & -\pi^2 & 2\pi \\ -4 & 2\pi & 4 - \pi^2 \end{pmatrix}.$$

Since this is an endfire array,

$$\begin{aligned} \mathbf{E} &= (\exp[-i(2\pi/\lambda)0], \exp[-i(2\pi/\lambda)(-\lambda/4)], \exp[-i(2\pi/\lambda)(-\lambda/2)])^T \\ &= (1, -i, -1)^T. \end{aligned}$$

And the \mathbf{A} matrix is found to be

$$\mathbf{A} = \begin{pmatrix} 1 & i & -1 \\ -i & 1 & i \\ -1 & -i & 1 \end{pmatrix}.$$

Then,

$$\alpha_{\text{opt}} = \mathbf{B}^{-1} \mathbf{E} = \frac{1}{8 - \pi^2} \begin{pmatrix} (8 - \pi^2) - 2\pi i \\ +\pi^2 i \\ -(8 - \pi^2) - 2\pi i \end{pmatrix}.$$

Expressing α_{opt} in polar form and normalizing it, we obtain amplitude coefficients (0.66, 1, 0.66) and phase coefficients (2.85, 0, 2.85).

$$\alpha_{\text{opt}}^* \mathbf{A} \alpha_{\text{opt}} = |V(\theta_0, \phi_0, \alpha_j)|^2 = \left(\frac{16 - 3\pi^2}{8 - \pi^2} \right)^2;$$

$$\alpha_{\text{opt}}^* \mathbf{B} \alpha_{\text{opt}} = \frac{16 - 3\pi^2}{8 - \pi^2}.$$

Therefore,

$$D_{\text{max}} = \frac{\alpha_{\text{opt}}^* \mathbf{A} \alpha_{\text{opt}}}{\alpha_{\text{opt}}^* \mathbf{B} \alpha_{\text{opt}}} = 7.26$$

$$\text{Max (DI)} = 10 \log_{10} D_{\text{max}} = 8.61 \text{ dB}$$

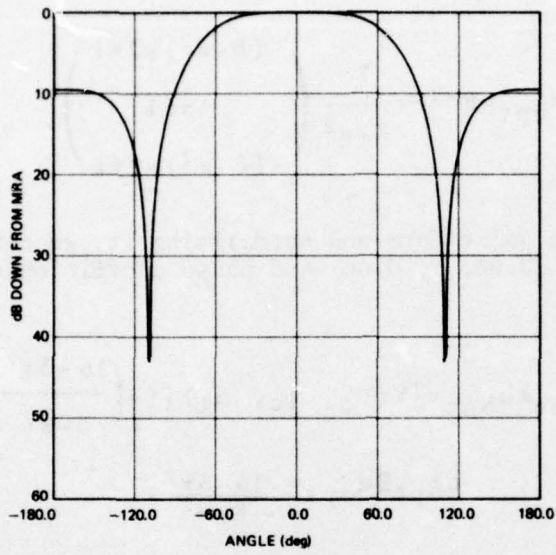
$$\text{(DI)}_{\text{unshaded}} = 4.77 \text{ dB}$$

$$\text{Improvement} = 3.84 \text{ dB}$$

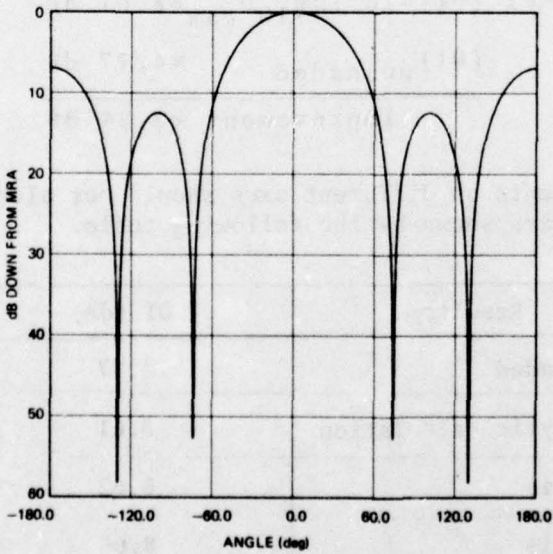
Placing these elements on different axes should not alter the DI. The numerical results are shown by the following table.

Results	DI (dB)
Unshaded	4.77
Analytic calculation	8.61
X-axis	8.62
Y-axis	8.65
Z-axis	8.62

Horizontal Beam:



HORIZONTAL BEAM PATTERN
PHI = 0.0 deg
ENDFIRE LINE ARRAY (3) - UNSHADED



HORIZONTAL BEAM PATTERN
PHI = 0.0 deg
ENDFIRE LINE ARRAY (3) - OPT SHADING

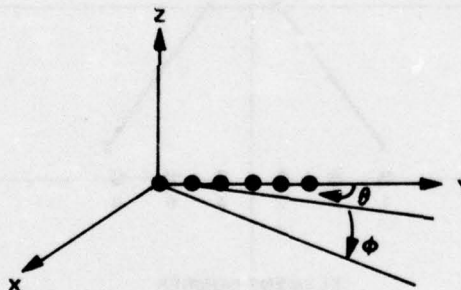
Beam Patterns

We examined whether or not changes occurred in the beam patterns. In this example, both the horizontal and vertical beam patterns seem to be improved somewhat. The plots of the endfire array on the Y-axis are shown on page 20.

EQUALLY SPACED ARRAY OF SIX ELEMENTS

Array Description

This is an endfire array of six equally spaced elements placed on the Y-axis that has the following configuration.

Input Considerations

Frequency = 4900 Hz

Plane wavefront is considered

Steering direction: (0, 0)

Since the procedure has already been described completely in the previous example, the **E** vector, **B** matrix, **B**⁻¹, and **A** vector calculations are omitted. We only list the normalized shading coefficients.

Numerical Calculations

Shading Coefficients-Maximum Directivity Index:

(a) $(1/4)\lambda$ spacing

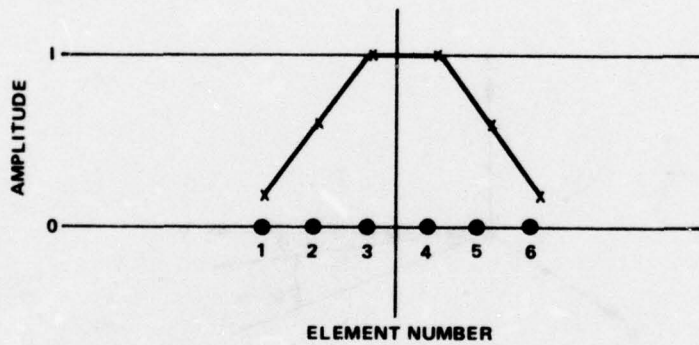
Element locations of this spacing are:

$$(x_j, y_j, z_j) = (0, \frac{j-1}{4}\lambda, 0), j=1, 2, \dots, 6.$$

The determined coefficients are:

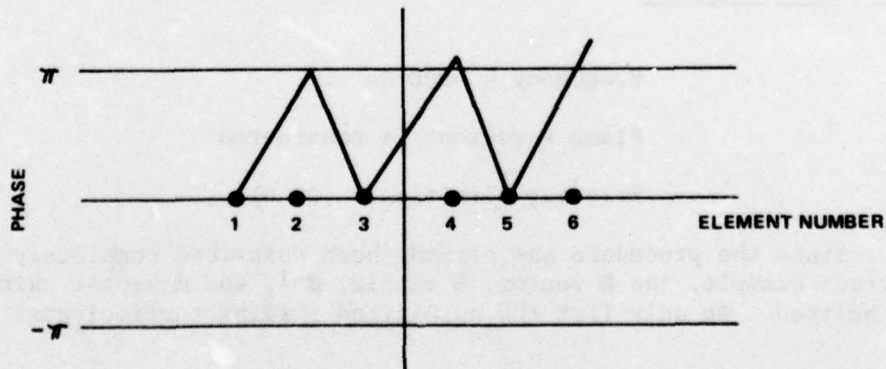
Amplitude coefficients:

$$(.21, .63, 1, 1, .63, .21)$$



Phase coefficients:

$$(-0.28, 3.01, 0, 3.27, 0.26, 3.55)$$



Using this set of coefficients we obtain the following results:

$$\text{Max DI} = 14.54 \text{ dB}$$

$$(\text{DI}) \text{ unshaded} = 7.78 \text{ dB}$$

$$\text{Improvement} = 6.76 \text{ dB}$$

(b) $(1/2)\lambda$ spacing

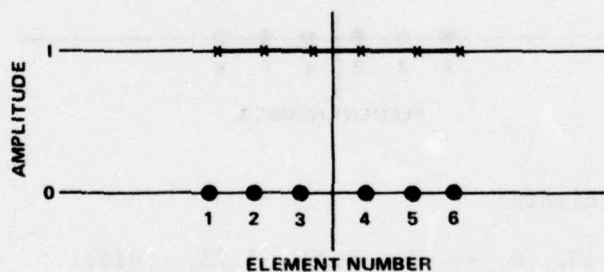
Element locations of this spacing are:

$$(x_j, y_j, z_j) = (0, \frac{j-1}{2}\lambda, 0), j=1, 2, \dots, 6.$$

The determined coefficients are:

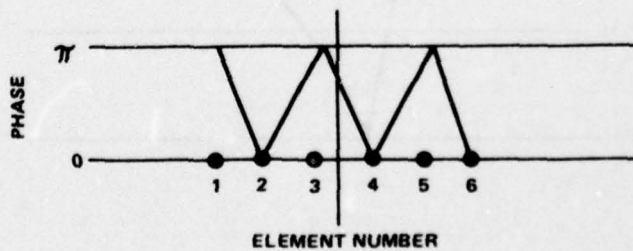
Amplitude coefficients:

$$(1, 1, 1, 1, 1, 1)$$



Phase coefficients:

$$(\pi, 0, \pi, 0, \pi, 0)$$



In this example, no improvement of DI was found due to element spacing.

(c) $(3/4)\lambda$ spacing

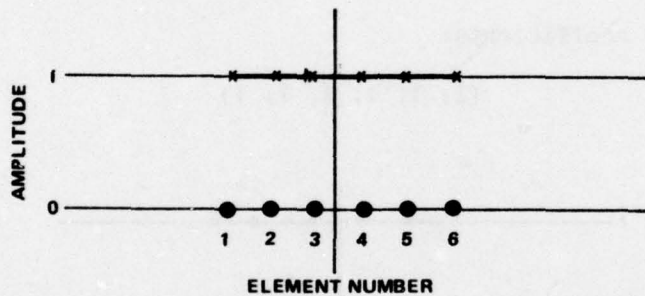
Element locations of this spacing are:

$$(x_j, y_j, z_j) = (0, \frac{3(j-1)\lambda}{4}, 0), j=1, 2, \dots, 6.$$

The determined coefficients are:

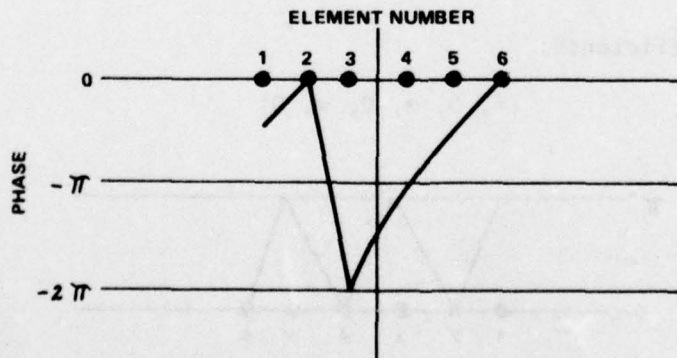
Amplitude coefficients:

$$(0.991, 1, 0.992, 0.992, 1, 0.991)$$



Phase coefficients:

$$(-.132, 0, -4.73, -3.29, -1.73, -.412)$$



Using this set of coefficients leads to a small improvement of DI, 0.18 dB.

Max DI = 7.96 dB

(DI) unshaded = 7.78 dB

Improvement = 0.18 dB

A Comparison with Tschebyscheff Technique: Using $(1/4)\lambda$ spacing produced a big improvement in DI by this technique. This result drew our interest to an investigation if the bandwidth over which gain could be achieved and to a comparison of results against existing well-known techniques. The Tschebyscheff technique has been selected for this comparison. In comparing the DI improvements and beam patterns, it was found that the Tschebyscheff technique is inferior to this technique, as shown in the following table.

DIRECTIVITY INDEX:

(a) $(1/4)\lambda$ spacing

Shading Function	Amplitude Shading Coefficients	DI (dB)	Improvement (dB)	
			Gain	Loss
Unshaded	(1, 1, 1, 1, 1, 1)	7.78		
Tschebyscheff*	(.3, .69, 1, 1, .69, .3)	7.04		0.74
This technique	(.21, .63, 1, 1, .63, .21)	14.54	6.76	

*The Tschebyscheff coefficients are obtained subject to the requirement that the side-lobe level is 30 dB.

(b) $(1/2)\lambda$ spacing

Shading Function	Amplitude Shading Coefficients	DI (dB)	Improvement (dB)	
			Gain	Loss
Unshaded	(1, 1, 1, 1, 1, 1)	7.78		
Tschebyscheff	(.3, .69, 1, 1, .69, .3)	7.04		0.74
This technique	(1, 1, 1, 1, 1, 1)	7.78	0	

(c) $(3/4)\lambda$ spacing

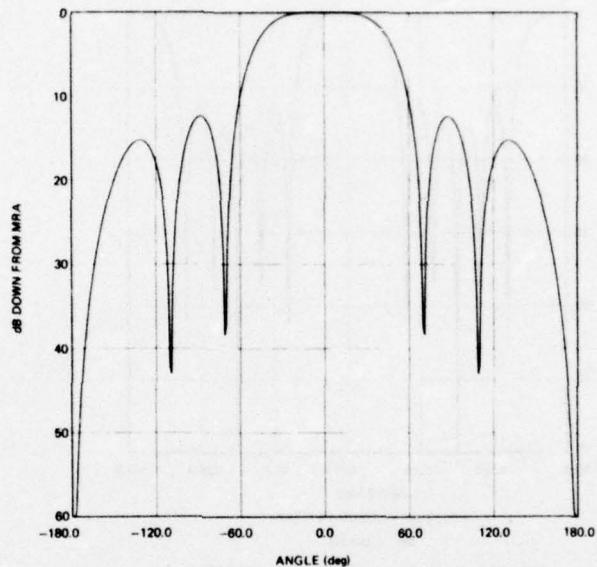
Shading Function	Amplitude Shading Coefficients	DI (dB)	Improvement (dB)
Unshaded	(1, 1, 1, 1, 1, 1)	7.78	
This technique	(.991, 1, .992, .992, 1, .991)	7.96	0.18

Examination of Bandwidth

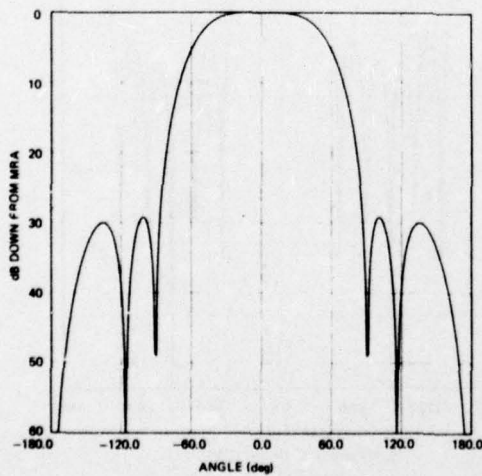
In carrying out the complete computations, we used a fixed frequency of 4900 Hz to determine a set of shading coefficients to maximize DI. The same set of coefficients were also used to calculate DI for different frequencies in order to determine the bandwidth. For an element spacing of $(1/4)\lambda$, based on a 4900 Hz center frequency, frequencies ranging from 3900 to 8000 Hz were evaluated in 100 Hz increments to examine the array bandwidth. Associated horizontal beam patterns at $f = 4300, 4900, 5800, 7100, \text{ and } 8100$ Hz were selected for presentation. For a spacing of $(3/4)\lambda$, based on a 4900 Hz center frequency, frequencies from 4400 to 5400 Hz were used; associated

Horizontal Beam Patterns

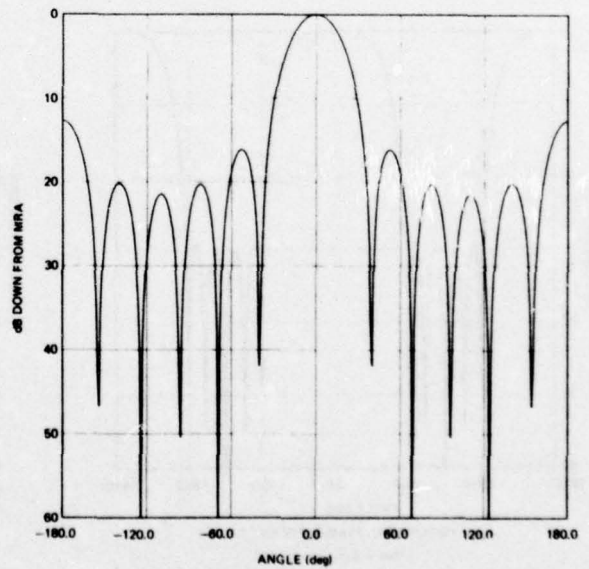
(a) $\lambda/4$ spacing



HORIZONTAL BEAM PATTERN
 PHI = 0.0 deg
 ENDFIRE LINE ARRAY (6) - $\lambda/4$ SPACING - UNSHADED



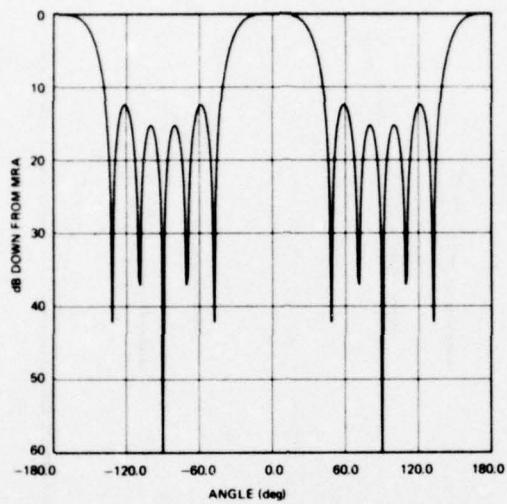
HORIZONTAL BEAM PATTERN
 PHI = 0.0 deg
 ENDFIRE LINE ARRAY (6) - $\lambda/4$ SPACING - TCHEBYSCHIEFF SHADING



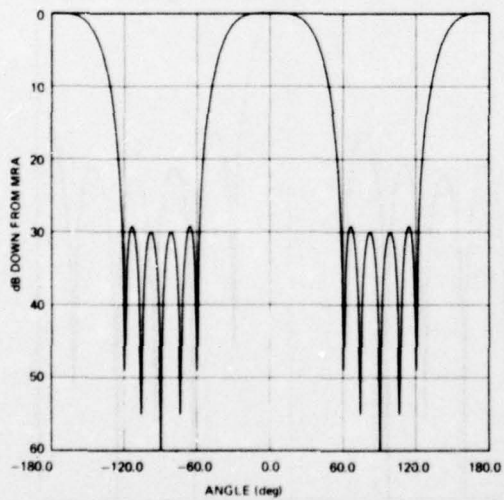
HORIZONTAL BEAM PATTERN
 PHI = 0.0 deg
 ENDFIRE LINE ARRAY (6) - $\lambda/4$ SPACING - OPT SHADING

TR 5375

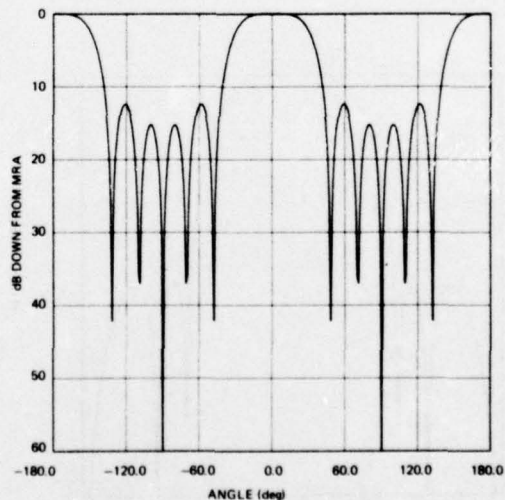
(b) $\lambda/2$ spacing



HORIZONTAL BEAM PATTERN
PHI = 0.0 deg
ENDFIRE LINE ARRAY (6) - $\lambda/2$ SPACING - UNSHADED

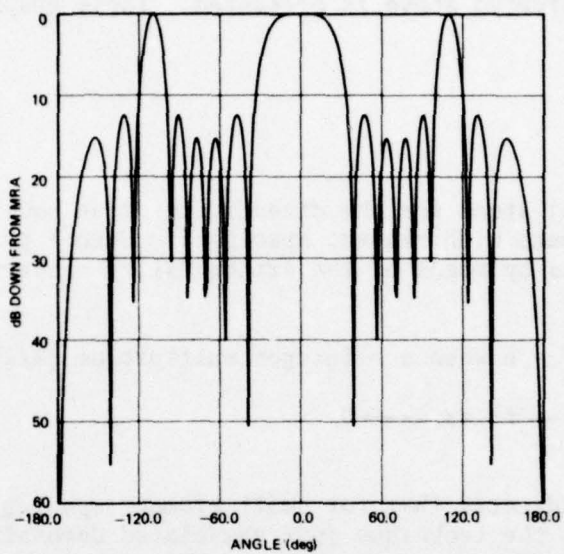


HORIZONTAL BEAM PATTERN
PHI = 0.0 deg
ENDFIRE LINE ARRAY (6) - $\lambda/2$ SPACING - TSHEBYSCHIEFF SHADING



HORIZONTAL BEAM PATTERN
PHI = 0.0 deg
ENDFIRE LINE ARRAY (6) - $\lambda/2$ SPACING - OPT SHADING

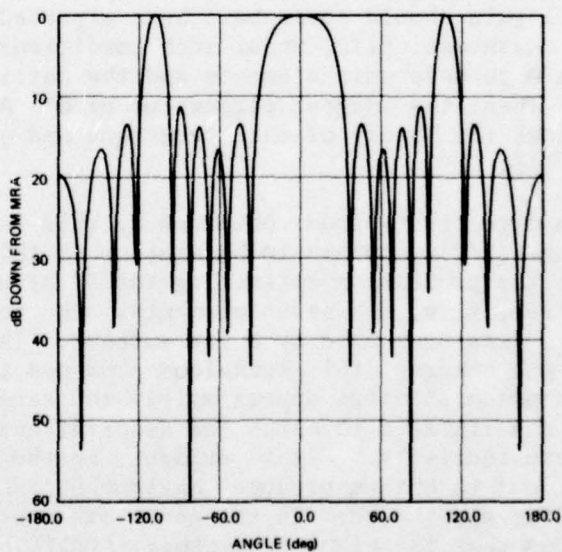
(c) $3\lambda/4$ spacing



HORIZONTAL BEAM PATTERN

PHI = 0.0 deg

ENDFIRE LINE ARRAY (6) - $3\lambda/4$ SPACING - UNSHADED - F = 4.9 kHz



HORIZONTAL BEAM PATTERN

PHI = 0.0 deg

ENDFIRE LINE ARRAY (6) - $3\lambda/4$ SPACING - OPT SHADING - F = 4.9 kHz

horizontal beam patterns are presented at frequencies of 4700, 4900, and 5100 Hz. A "Frequency vs DI" graph based on the two spacings, $(1/4)\lambda$ and $(3/4)\lambda$, considered above is presented. These graphs are labeled figures 2 and 3.

Discussion

Let $D(n, s)$ stand for the directivity of an equally-spaced line array of n elements with element spacing s . Uzkov¹ proved the following important results by means of the orthogonality properties of inner products:

$$D(n, s) \left\{ \begin{array}{l} = n \text{ when } s = \text{integer multiple of } (1/2)\lambda \quad (\text{A}) \\ \longrightarrow n^2 \text{ as } s \longrightarrow 0 \quad (\text{B}) \end{array} \right.$$

Uzkov's proof indicates that for small element spacing, high directivity can be expected; the technique just enunciated demonstrated that such a high directivity index can be achieved. The results in the previous section, obtained by using a $(1/4)\lambda$ spacing, clearly support the above statements.

When a $(1/2)\lambda$ spacing is used in the example, no DI gain is seen. In such case, a DI gain should never have been expected according to Uzkov's results. Mathematically, under such conditions, our technique determines matrix **A** to have unit elements and the matrix **B** to be an identity matrix. Then, the largest eigenvalue of $\mathbf{B}^{-1} \mathbf{A}$ is P_n , which equals n ; this shows the beauty of this technique and justifies Uzkov's proof of formula (A).

The maximum directivity index obtained by this technique by using an element spacing $>(1/2)\lambda$ appears to be similar to those obtained by Pritchard^{15,16} in the process of optimizing the DI of equally-spaced line arrays of three, five, and seven elements. The terminology, "superdirectivity," has been used by a few authors. In fact, for other than half-wavelength spacing, this technique produces a narrower main lobe and produces phase shadings approximately the reverse of adjacent elements. These results seem to match the descriptions given by Urick²⁶ for "superdirectivity." It is evident, in the absence of round-off errors, our technique produces maximum DI (MDI); this would mean that our MDI is also "super" in the sense of superdirectivity. Pritchard concluded that for element spacings $>(1/2)\lambda$ there is little difference between the maximum DI and the unshaded DI. His conclusion confirms our findings for $(3/4)\lambda$ spacing.

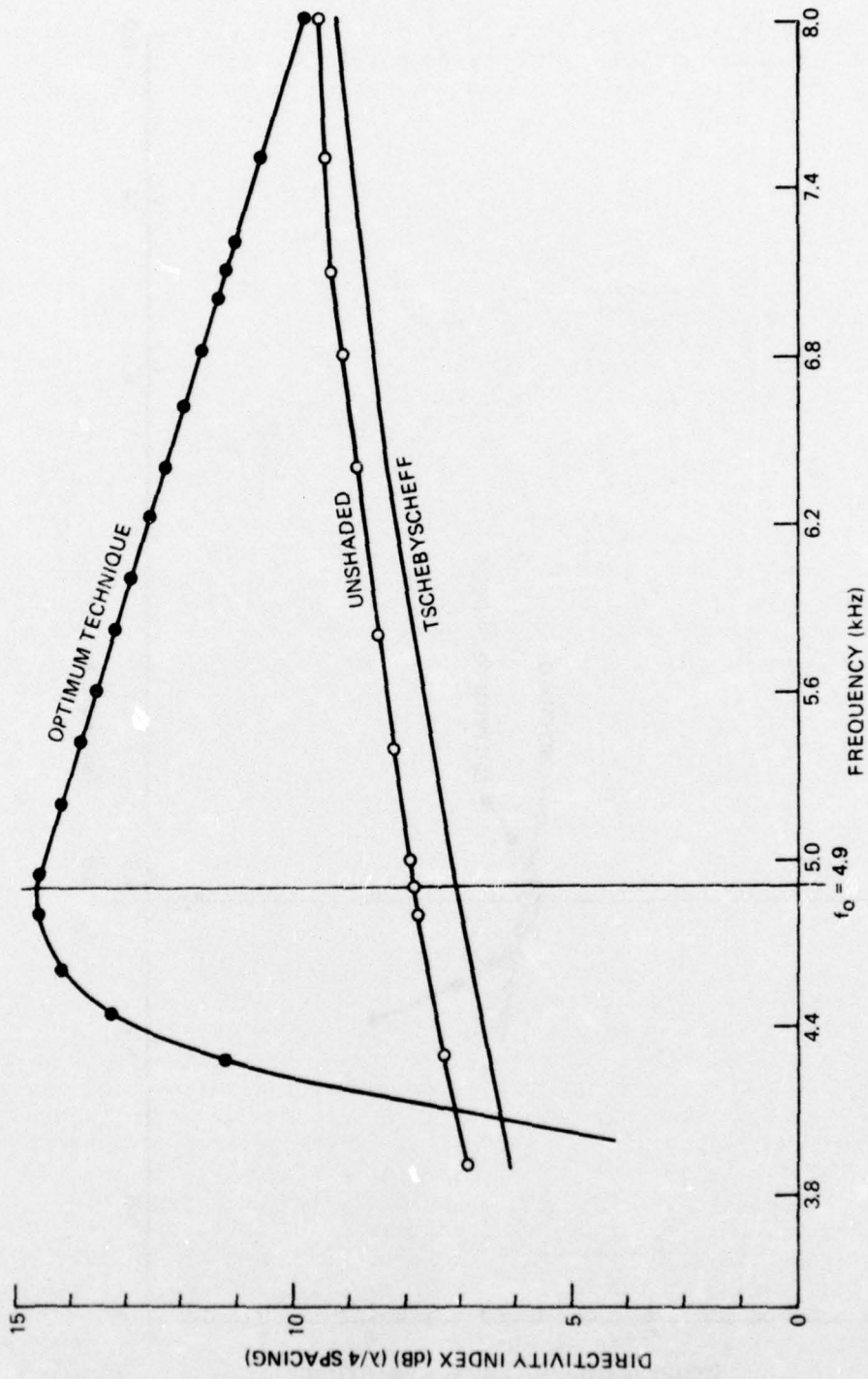


Figure 2.

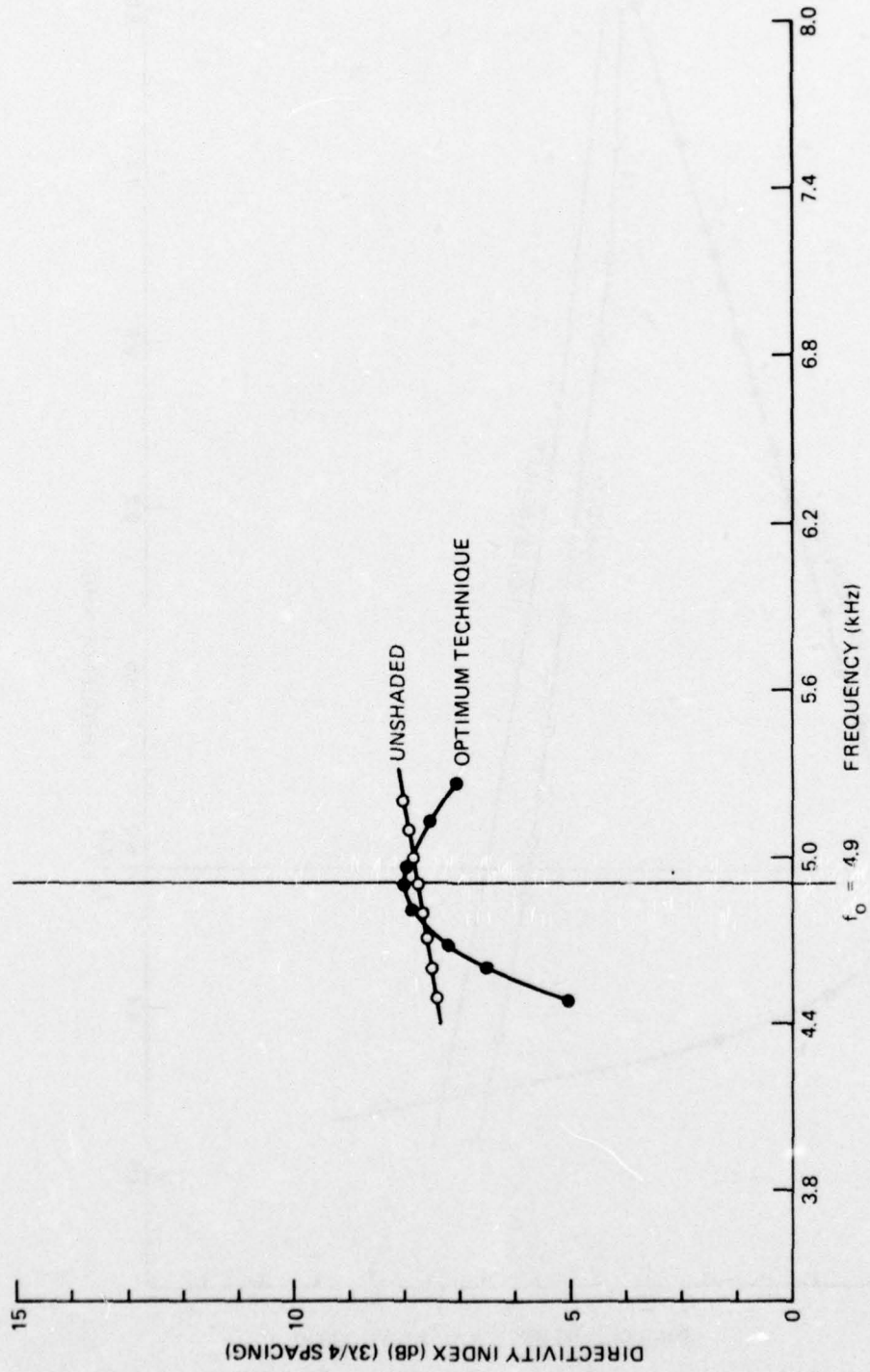
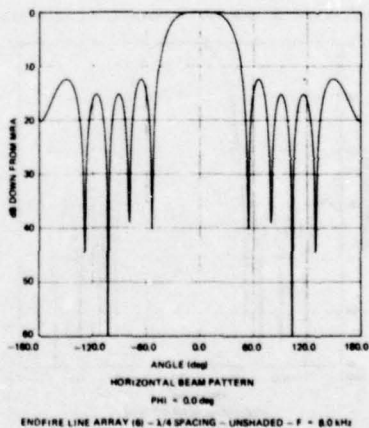
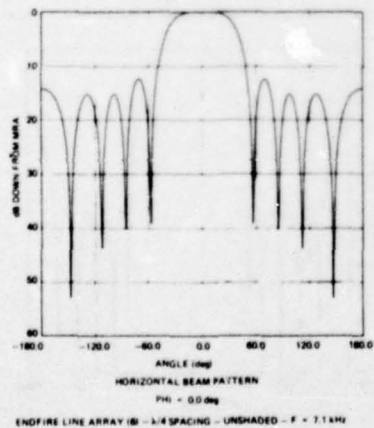
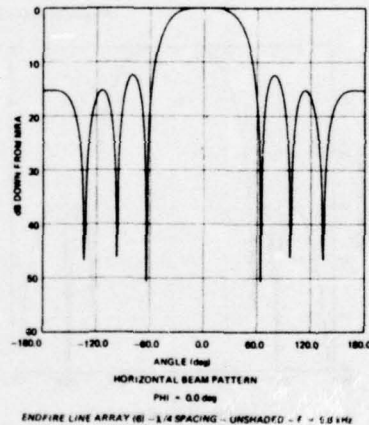
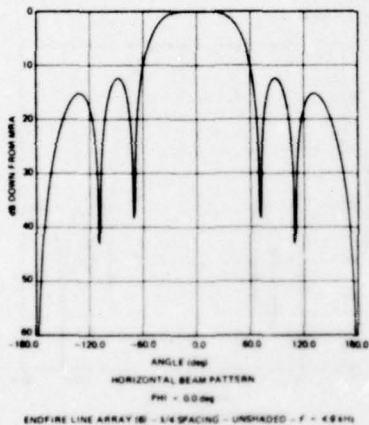
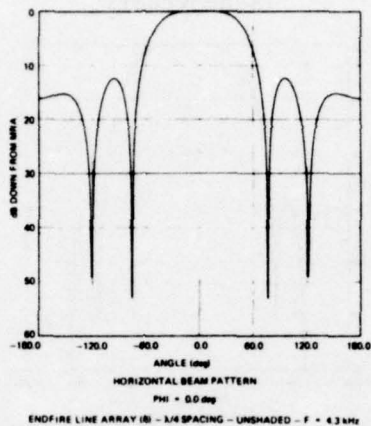
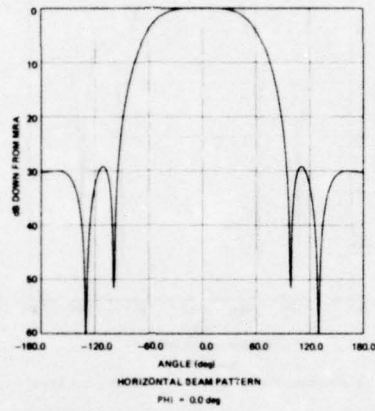


Figure 3.

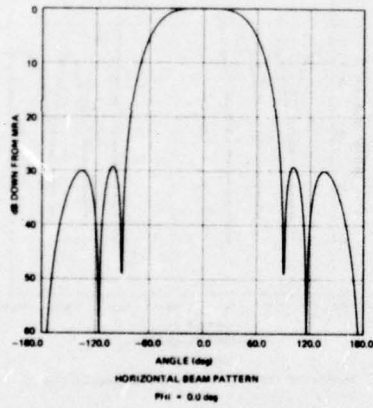
Horizontal Beam Patterns ($\lambda/4$ spacing)
Unshaded



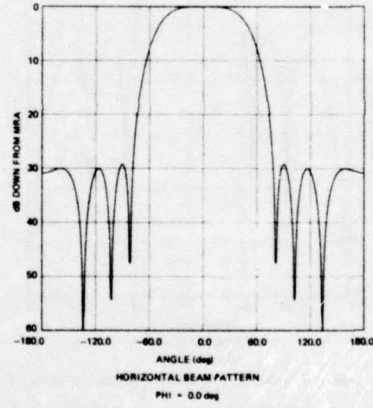
Horizontal Beam Patterns ($\lambda/4$ spacing)
Tschebycheff



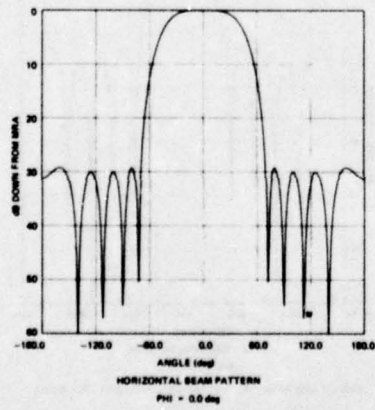
ENDFIRE LINE ARRAY (E) - $\lambda/4$ SPACING - TSCHEBYSCHIEFF SHADING - F = 4.3 kHz



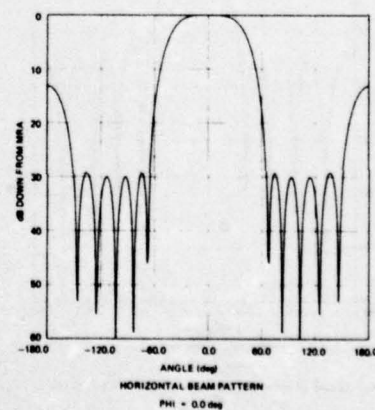
ENDFIRE LINE ARRAY (E) - $\lambda/4$ SPACING - TSCHEBYSCHIEFF SHADING - F = 4.8 kHz



ENDFIRE LINE ARRAY (E) - $\lambda/4$ SPACING - TSCHEBYSCHIEFF SHADING - F = 5.8 kHz

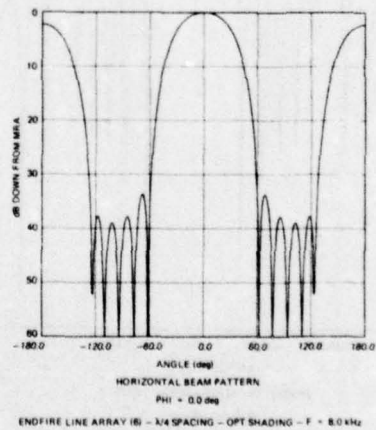
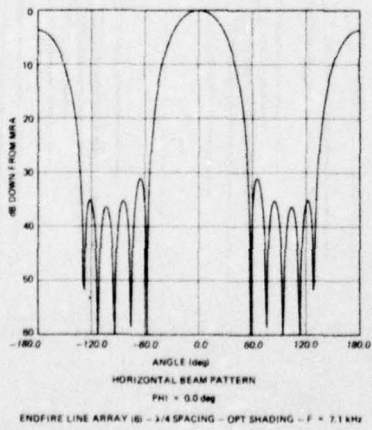
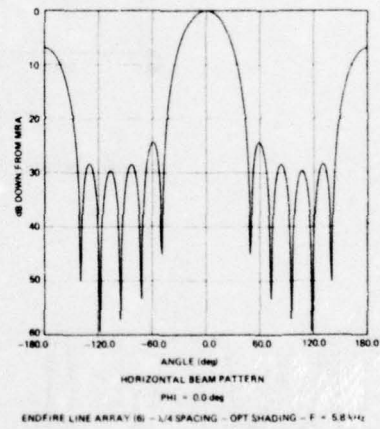
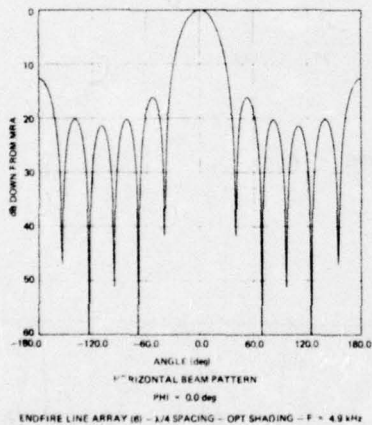
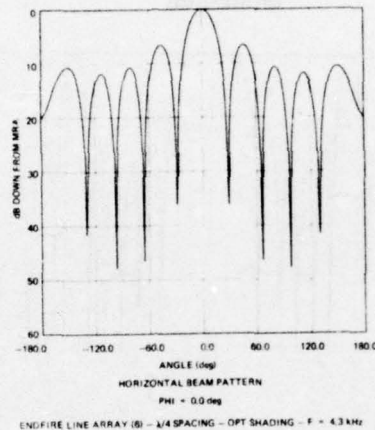


ENDFIRE LINE ARRAY (E) - $\lambda/4$ SPACING - TSCHEBYSCHIEFF SHADING - F = 7.1 kHz

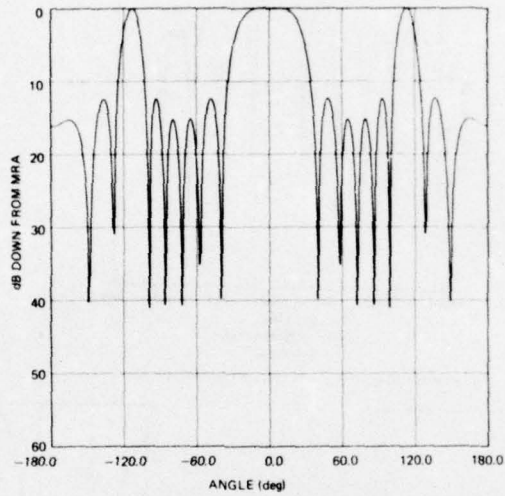


ENDFIRE LINE ARRAY (E) - $\lambda/4$ SPACING - TSCHEBYSCHIEFF SHADING - F = 8.8 kHz

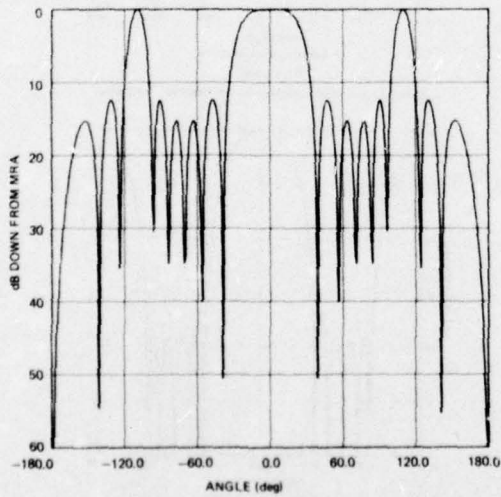
Horizontal Beam Patterns ($\lambda/4$ spacing)
This Technique



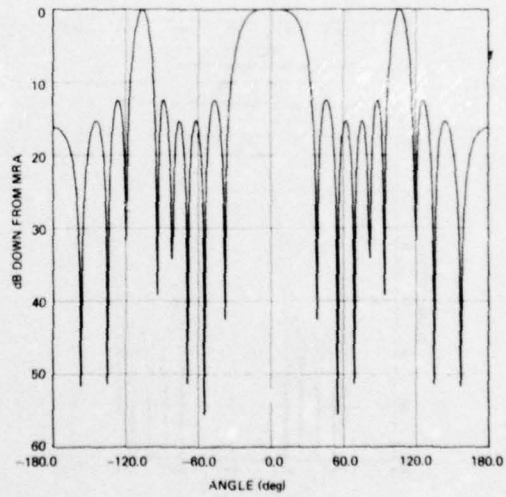
Horizontal Beam Patterns ($3\lambda/4$ spacing)
Unshaded



HORIZONTAL BEAM PATTERN
PHI = 0.0 deg
ENDFIRE LINE ARRAY (6) - $3\lambda/4$ SPACING - UNSHADED - F = 4.7 kHz

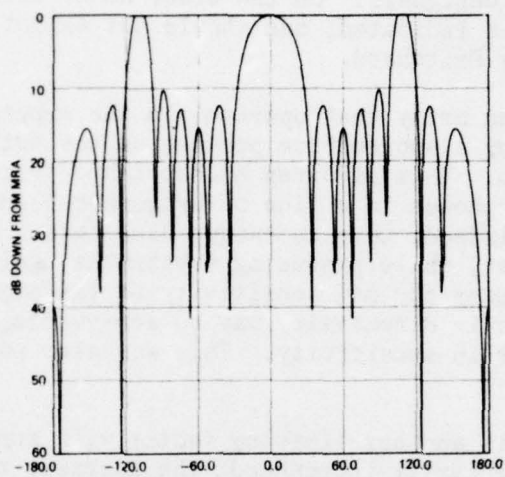


HORIZONTAL BEAM PATTERN
PHI = 0.0 deg
ENDFIRE LINE ARRAY (6) - $3\lambda/4$ SPACING - OPT SHADING - F = 4.9 kHz

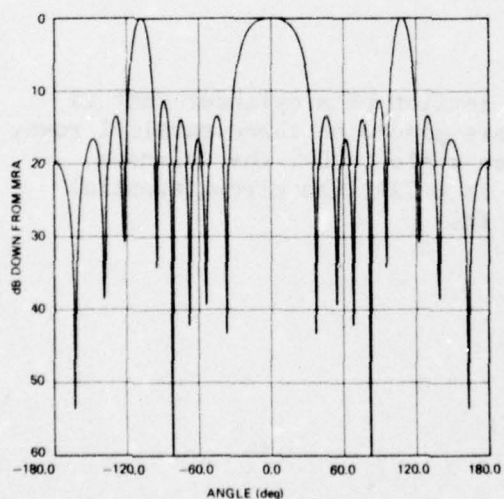


HORIZONTAL BEAM PATTERN
PHI = 0.0 deg
ENDFIRE LINE ARRAY (6) - $3\lambda/4$ SPACING - OPT SHADING - F = 5.1 kHz

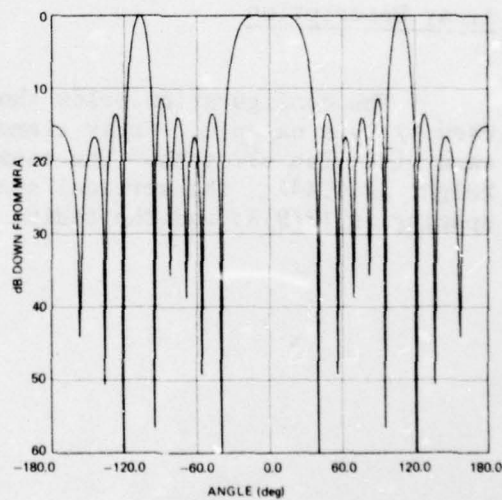
horizontal Beam Patterns ($3\lambda/4$ spacing)
This Technique



HORIZONTAL BEAM PATTERN
PHI = 0.0 deg
ENDFIRE LINE ARRAY (6) - $3\lambda/4$ SPACING - OPT SHADING - F = 4.7 kHz



HORIZONTAL BEAM PATTERN
PHI = 0.0 deg
ENDFIRE LINE ARRAY (6) - $3\lambda/4$ SPACING - OPT SHADING - F = 5.1 kHz



HORIZONTAL BEAM PATTERN
PHI = 0.0 deg
ENDFIRE LINE ARRAY (6) - $3\lambda/4$ SPACING - UNSHADED - F = 4.9 kHz

On the examination of bandwidth, using $(1/4)\lambda$ spacing, we found a wide frequency band of 4000 Hz; therefore, these results should be of interest to array designers. On the other hand, with $(3/4)\lambda$ spacing, a small gain of DI is indicated; one should not expect a wide frequency band as implied by Pritchard.

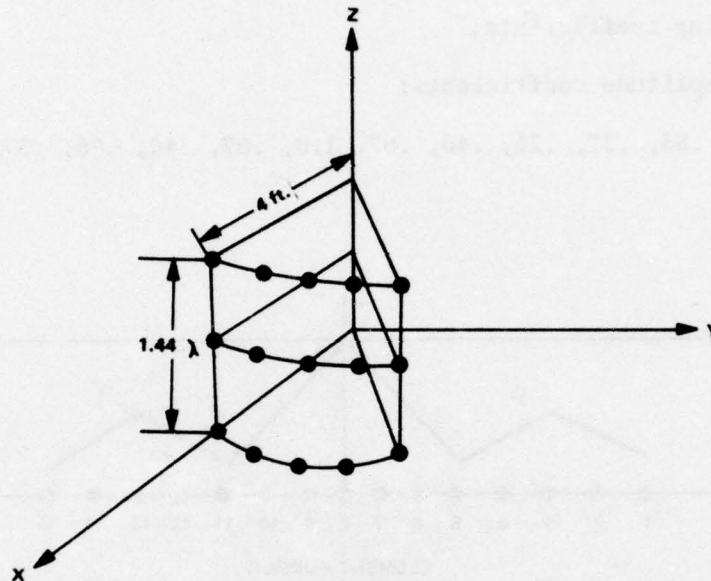
To design an array that operates in the superdirective mode, it is necessary to employ a subtractive process on the output of closely spaced hydrophones. This is often accomplished by reversal of the phase of alternate hydrophones in a line of hydrophones spaced at a $1/4$ wavelength interval; indeed, this technique does this. Unfortunately the subtractive process, while producing substantial gains in directivity, significantly reduces the net sensitivity of the super-directive array. Moderate increases in directivity may be achievable, however, with a moderate sacrifice in sensitivity. This was also pointed out by Pritchard.^{15,16}

Bandwidth is another limiting factor with superdirective arrays. The more superdirectivity introduced, the narrower the bandwidth of the array with respect to the bandwidth that would be available with conventional wider interhydrophone spacing.

A CYLINDRICAL ARRAY OF 15 ELEMENTS

Array Description

The configuration below shows a section of a cylinder that is used by this example. Array elements are placed on three parallel rows, each with five elements. The separation angle is 50° ; the cylinder height is 1.44λ ; the vertical spacing is 0.72λ ; the circumferential spacing is $(\pi/9)\lambda$; and the radius is 4 ft.



Input Considerations

Element locations: $(x_j, y_j, z_j) = (\gamma \cos \theta_j, \gamma \sin \theta_j, z_j)$
 $\theta_j = 5^\circ (j-1), j=1, 2, \dots, 5$

Frequency: 3500 Hz

Plane wavefront is considered

Steering direction: $(80^\circ, 0^\circ)$

$$RV(\theta, \phi) = \begin{cases} 1 & -1^\circ < \phi < 1^\circ \\ 0 & \text{elsewhere} \end{cases}$$

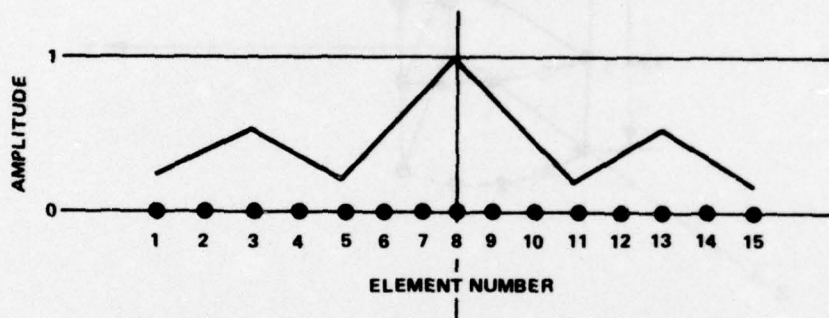
TR 5375

Numerical Results - Maximum RI and DI

Shading coefficients:

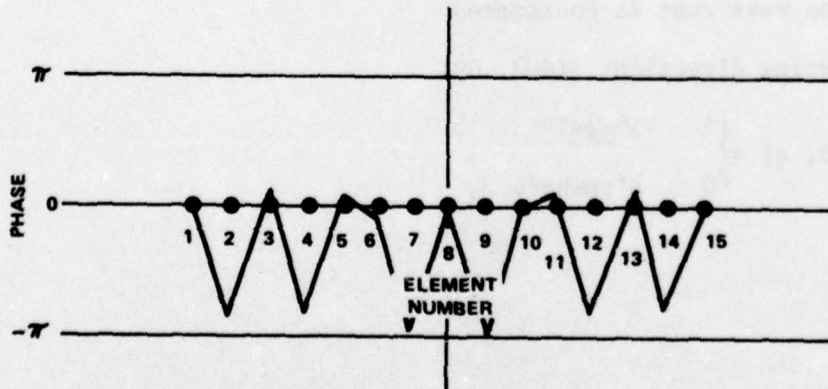
Amplitude coefficients:

(.26, .37, .53, .37, .26, .40, .67, 1.0, .67, .40, .26, .37, .53, .37, .26)



Phase coefficients:

(.11, -2.82, .19, -2.82, .11, -.02, -3.06, 0, -3.06, -.02, .11, -2.82, .19, -2.82, .11)



Using this set of coefficients to maximize RI and DI leads to the following improvements.

Shading Functions	DI (dB)	RI (dB)
Unshaded	10.29	5.91
This technique	11.81	7.19
Improvement	1.52	1.28

Note that any improvement is worthwhile. In some instances the improvement may be greater. Above is only an example.

Discussions

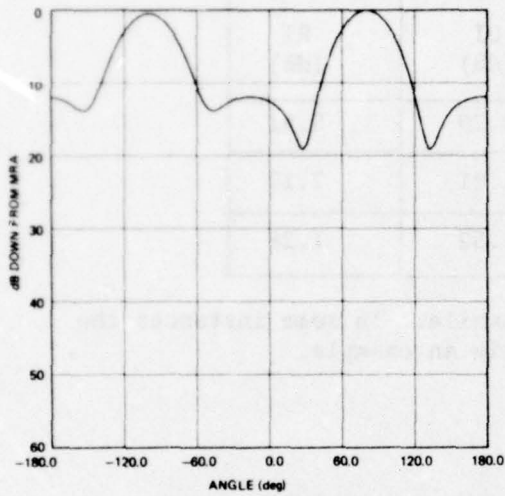
A noticeable RI and DI gain is produced as a result of this example. In carrying out the computations, we observed that the reverberation function, $RV(\theta, \phi)$, is defined in a small sector that is a part of the main lobe. Even though the main lobe in that small sector is narrowed after the maximization is done, no control can be assured for the beam patterns elsewhere outside the sector. Often, when the vertical main lobe is wider than the reverberation sector, undesirable beam patterns can be produced. Under such condition, even though the RI is maximized, the DI may be deteriorated. This occurrence should be considered unacceptable. To remedy this situation, a procedure was modified to improve the RI subject to the requirement that not only the RI and DI can be improved simultaneously but also the beam patterns can be improved. This approach is tried to vary the reverberation sector to cover the main lobe and to improve RI and DI. Six reverberation sectors are tried for the above example; the reverberation function maintains the original definition. These beam patterns are displayed below. Horizontal beams all show acceptable patterns, but the vertical beam patterns deteriorate with narrowing reverberation sectors (indicated by [,]).

The directivity index values are also examined; they deteriorate with the narrowing reverberation sector.

Beam Patterns:

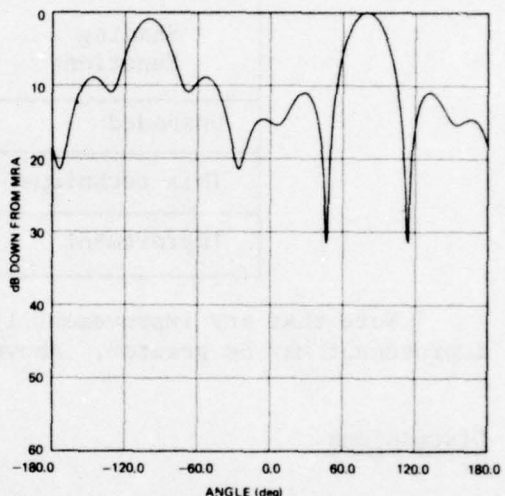
Horizontal Beam Patterns

Unshaded



HORIZONTAL BEAM PATTERN
PHI = 0.0 deg
CYLINDER (15) - (80, 0) - UNSHADED

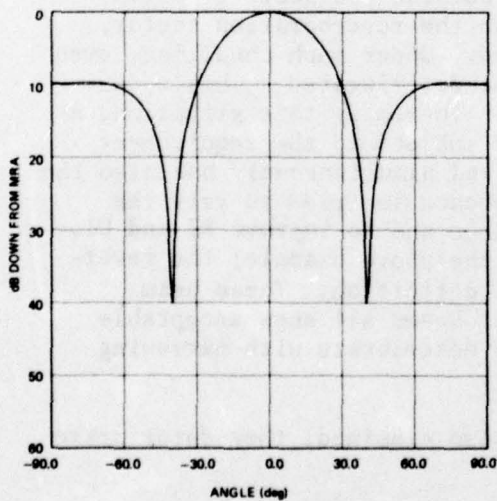
This Technique



HORIZONTAL BEAM PATTERN
PHI = 0.0 deg
CYLINDER (15) - (80, 0) - OPT SHADING

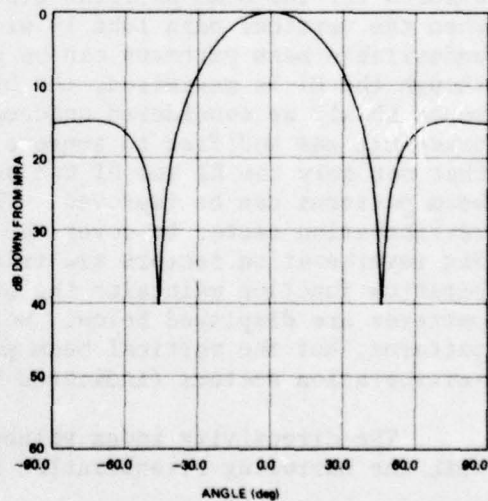
Vertical Beam Patterns

Unshaded

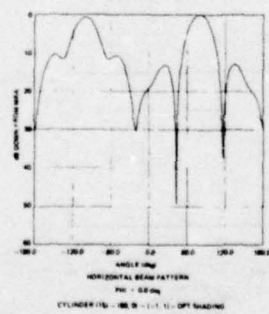
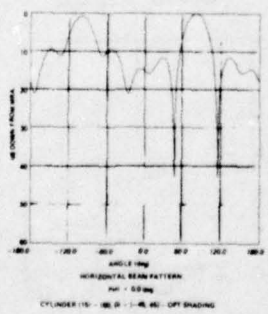
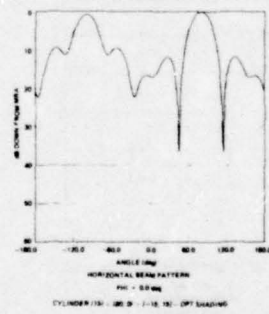
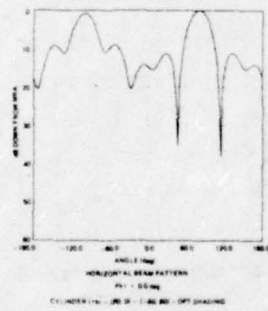
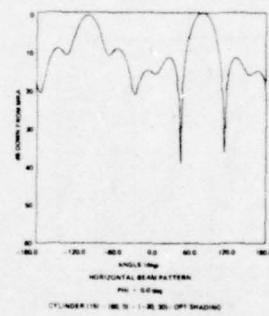
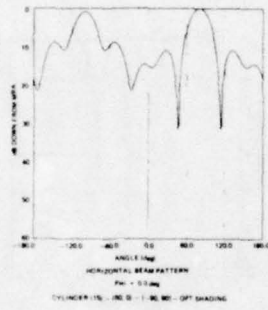
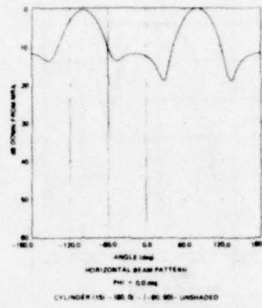


VERTICAL BEAM PATTERN
THETA = 80.0 deg
CYLINDER (15) - (80, 0) - UNSHADED

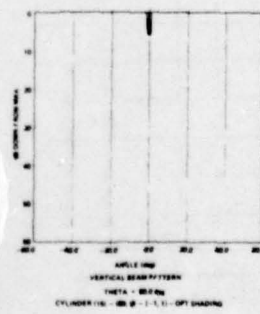
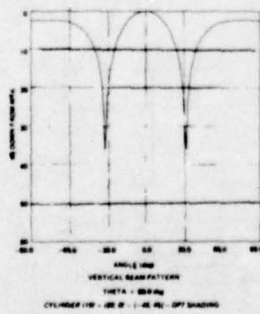
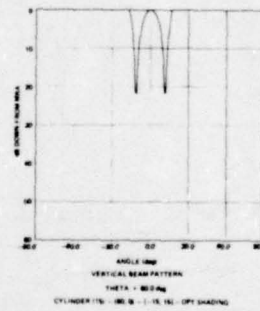
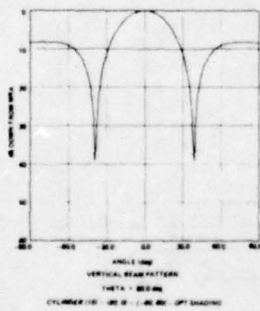
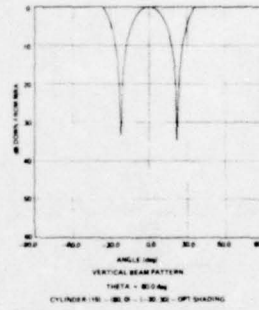
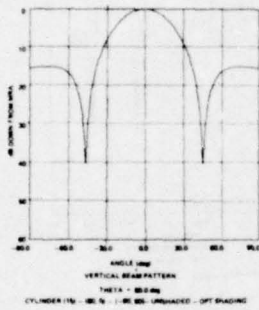
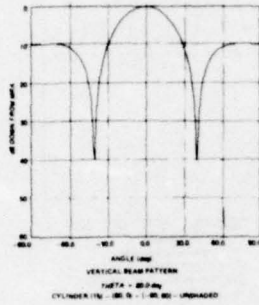
This Technique



VERTICAL BEAM PATTERN
THETA = 80.0 deg
CYLINDER (15) - (80, 0) - OPT SHADING



Horizontal



Sector \ Index	RI (dB)	DI (dB)
Unshaded	5.91	10.29
$[-90^\circ, 90^\circ]$	7.19	11.81
$[-60^\circ, 60^\circ]$	7.18	11.41
$[-45^\circ, 45^\circ]$	7.19	9.31
$[-30^\circ, 30^\circ]$	7.20	2.55
$[-15^\circ, 15^\circ]$	7.23	*
$[-1^\circ, 1^\circ]$	8.34	*
*unreasonable results		

This example represents a small array; the computation time does not impose a problem. For large arrays, the reduction of computation time should be seriously taken into consideration. The saving can be realized by a compromise on RI and DI gain. The above results seem to suggest that the sector $[-60^\circ, 60^\circ]$ may be a good choice for this example. Now, the question arises: In general, what is a reasonable sector to choose to maximize RI and at the same time to minimize the computations? It seems that a good choice is the smallest interval containing the vertical main lobe. In some cases, the vertical main lobe is already narrow; then this choice can save a great deal of computation time.

FUTURE RESEARCH

The complete optimization of RI and DI, in fact, involves three domains of analysis: applied mathematics, computer science, and engineering-physics. The solution of the pertinent problems in each domain will allow hardware development applying the subject technique to be undertaken. This paper solved only the applied mathematics problem. Before the actual applications can be carried out to solve the engineering-physics problems, it is necessary to solve the problem in computer science. It is evident that the immediate need to carry on the research is a computer model with desirable options. The practical consideration is an automation of a set of existing computer

programs plus options subject to machine memory capacity. Extension of this model should handle arrays of any size that will be the most general model. Design of such a model is systematic. For large arrays, when the number of array elements is large enough to produce a large \mathbf{B} matrix that exceeds the allowable machine memory capacity, the computations are expected to be extremely long and need to be handled in a special manner.

A complete examination of the optimum properties of existing sonar arrays should be interesting and profitable.

This technique can be applied to produce valuable results that can lead to the future design of optimal arrays.

CONCLUSIONS

An effective technique based on matrix theory has been developed to apply an elegant theory to maximize RI and DI. Evidently, the numerical results demonstrated its validity. Some engineering and physical considerations are not examined in this paper. It is believed that this technique is general enough to be applied extensively to any type of sonar array without restriction.

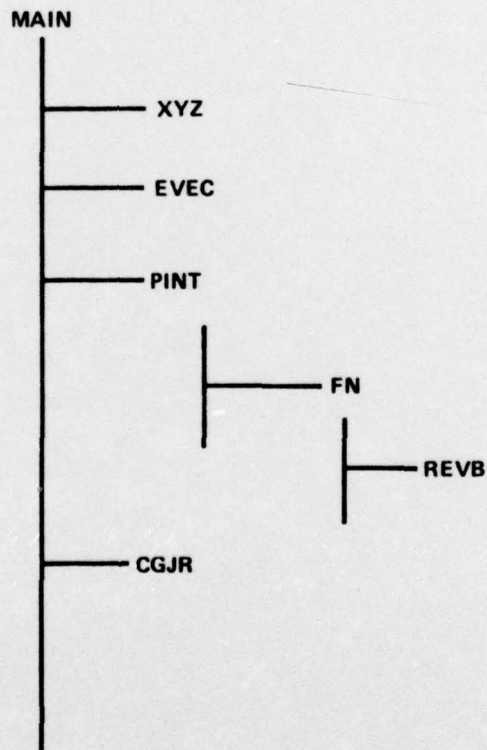
Maximizing RI and DI is considered important. Also important is the minimization of computations for large arrays. Concerning minimization of computations, special treatment ought to be considered for special problems. For a large array, such as equally spaced line arrays, the \mathbf{B} matrix to be determined takes a special representation, a Toeplitz matrix (Zohar²⁷). Existing special algorithms are recommended to invert this type of matrix to gain computational efficiency.

This technique not only can be considered useful for future array designs, but also can be used to examine the optimum property of present existing sonar arrays. If an existing array has already possessed optimum property, then no improvement can be expected. This technique will indicate so. In this case, the matrix \mathbf{A} becomes a matrix of unit elements and \mathbf{B} becomes an identity matrix.

This technique depends upon element spacings as well as steering directions. Numerical results of equally spaced line arrays with small spacing show superdirectivity. Cheng,^{5,6} in maximizing directive gain for circular and elliptical arrays, concluded that for small element separations a supergain situation results under optimum gain conditions. The trend of numerical results seems to indicate that RI and DI can be maximized where the element separations are very small.

APPENDIX

A set of seven FORTRAN V computer programs have been developed to implement this technique. Their interdependence is described by the diagram below. Calculations are performed on the UNIVAC 1108, using single-precision arithmetic. Compilation is done by the EXEC 8 system.



MAIN	commands the control
XYZ	generates element locations
EVEC	calculates E vector
PINT	performs two-dimensional numerical integration

TR 5375

FN computes the integrand
REVB defines the reverberation function
CGJR inverts Hermitian matrix B.

Outputs are a set of normalized amplitude coefficients and associated phase coefficients.

MAIN

```

PARAMETER NR=30
COMPLEX B(NR,NR),EV(NR),BV(NR),V(NR)
DIMENSION XH(NR),YH(NR),ZH(NR),X(NR),Y(NR)
DATA P1,ONE,ZERO/3.1415926535,1.0,0.0/
DATA BV/NR*(0.0,0.0)/
DATA VELCTY/4900.0/
NAMELIST /INPUTS/HHZ,HVT,LOWH,LIMH,LOWV,LIMV,MANYH,INDEX,F,VELCTY,
$ IXYZ,L,M,N,XSPACE,YSPACE,ZSPACE,THEM,PHIM,IDR/
NN=NR
1 READ(3,INPUTS,ERR=1000,END=1000)
WL=VELCTY/F
CALL XYZ(IXYZ,XH,YH,ZH,L,M,N,XSPACE,YSPACE,ZSPACE,X0,Y0,Z0,LMN)
DO 50 I=1,LMN
WRITE (4,100) I,XH(I),YH(I),ZH(I)
50 CONTINUE
100 FORMAT(10X,I3,3(4X,E15.8))
CALL EVEC(THEM,PHIM,XH,YH,ZH,LMN,WL,EV)
101 FORMAT(/10X,'E VECTOR--'/)
WRITE (4,101)
WRITE (4,103) (EV(J),J=1,NN)
103 FORMAT(10(/1X,6(E15.8,2X)))
DO 10 I=1,LMN
DO 10 J=1,LMN
IF(I.NE.J) GO TO 9
B(I,J)=CMPLX(ONE,ZERO)
GO TO 10
9 MANYH=1
CALL PINT(HHZ,HVT,LOWH,LIMH,LOWV,LIMV,MANYH,XH,YH,ZH,I,J,0,L,IDR,
$A)
MANYH=1
CALL PINT(HHZ,HVT,LOWH,LIMH,LOWV,LIMV,MANYH,XH,YH,ZH,I,J,1,VL,IDR,
$S)
B(I,J)=CMPLX(A,S)
10 CONTINUE
DO 110 I=1,LMN
DO 110 J=1,LMN
110 B(J,I)=CMPLX(REAL(B(I,J)),-AIMAG(B(I,J)))
WRITE (4,102)
102 FORMAT(/10X,'1ST ROW OF B MATRIX--'//)
WRITE (4,103) (B(1,J),J=1,NN)
201 FORMAT(1H1)
WRITE (4,201)
DO 3 I=1,NN
3 CONTINUE
V(1)=(1.0,0.0)
CALL CGJR(B,NN,NN,NN,NN,$1000,JC,V)

```

Copy available to DDC does not
 permit fully legible reproduction

TR 5375

```
DO 5 I=1,NN
5 CONTINUE
DO 209 I=1,NN
DO 208 J=1,NN
BV(I)=BV(I)+B(I,J)*EV(J)
208 CONTINUE
X(I)=SQRT(REAL(BV(I))**2+AIMAG(BV(I))**2)
Y(I)=ATAN2(AIMAG(BV(I)),REAL(BV(I)))
WRITE (4,210) I,BV(I),X(I),Y(I)
1100 FORMAT(11X,2(E15.8,2X))
PP=X(I)*COS(Y(I))
QQ=X(I)*SIN(Y(I))
WRITE (4,1100) PP,QQ
209 CONTINUE
210 FORMAT(2X,13,5X,'(',2(E15.8,2X),')',10X,'MAGNITUDE=',E15.8,10X,
$'ANGLE=',E15.8)
U=0.0
DO 11 I=1,NN
IF(ABS(X(I)) .LE. U) GO TO 11
U=ABS(X(I))
11 CONTINUE
12 FORMAT(/15X,40(1H*)//5X,'SHADING COEFFICIENTS AFTER NORMALIZATION'
//10(/1X,3(E15.8,4X)))
DO 13 I=1,NN
X(I)=X(I)/U
13 CONTINUE
WRITE (4,12) (X(J),J=1,NN)
GO TO 1
1000 STOP
END
```

Copy available to DDC does not
permit fully legible reproduction.

XYZ

```

SUBROUTINE XYZ(IXYZ,XH,YH,ZH,L,M,N,XSPACE,YSPACE,ZSPACE,XO,YO,ZO,
3LEN)
DIMENSION XH(1),YH(1),ZH(1)
DATA KAO/0.01745329/
LMN=L*M*N
LMN=30
IF(IXYZ .NE. 0) GO TO 8
IF(XSPACE .LE. 0.0) GO TO 3
IXO=0
XO=FLOAT(L-1)*XSPACE/2.0
DO 1 I=1,L
DO 11 J=1,M
DO 2 K=1,N
IXO=IXO+1
XH(IXO)=FLOAT(I-1)*XSPACE-XO
21 CONTINUE
11 CONTINUE
1 CONTINUE
3 IF(YSPACE .LE. 0.0) GO TO 5
IYO=0
YO=0.0
DO 4 J=1,M
DO 14 I=1,L
DO 24 K=1,N
IYO=IYO+1
YH(IYO)=FLOAT(J-1)*YSPACE-YO
24 CONTINUE
14 CONTINUE
4 CONTINUE
5 IF(ZSPACE .LE. 0.0) GO TO 6
IZO=0
ZO=FLOAT(N-1)*ZSPACE/2.0
DO 7 K=1,N
DO 17 I=1,L
DO 27 J=1,M
IZO=IZO+1
ZH(IZO)=FLOAT(K-1)*ZSPACE-ZO
27 CONTINUE
17 CONTINUE
7 CONTINUE
6 RETURN

```

COPY AVAILABLE TO DDC DOES NOT
PERMIT FULLY LEGIBLE PRODUCTION

TR 5375

```
8 CONTINUE
  IZ=-2
30 IZ=IZ+2
  IF (IZ .GT. 4) GO TO 32
  JZ=5*IZ
  DO 31 I=1,10
    XH(I+JZ)=4.*COS(5.*(I-1)*RAD)
    YH(I+JZ)=4.*SIN(5.*(I-1)*RAD)
    ZH(I+JZ)=IZ
31 CONTINUE
  GO TO 30
32 CONTINUE
  XO=0.0
  YO=0.0
  ZO=0.0
  DO 9 I=1,LMN
    XU=XO+XH(I)
    YU=YO+YH(I)
    ZU=ZO+ZH(I)
9 CONTINUE
  XU=XU/FLOAT(LMN)
  YU=YU/FLOAT(LMN)
  ZU=ZU/FLOAT(LMN)
  DO 10 I=1,LMN
    XH(I)=XH(I)-XO
    YH(I)=YH(I)-YO
    ZH(I)=ZH(I)-ZO
10 CONTINUE
  RETURN
  END
```

Copy available to DDC does not
permit fully legible reproduction

EVEC

```

SUBROUTINE EVEC(TH,PH,LMN,XH,YH,ZH,WM,EV)
DIMENSION XH(1),YH(1),ZH(1)
COMPLEX EV(1)
DATA PI,DEG/6.283185307,0.1745329E-01/
TH=TH*DEG
PH=PH*DEG
ALPHA=COS(PH)*SIN(TH)
BETA=COS(PH)*COS(TH)
GAMMA=-SIN(PH)
DO 1 I=1,LMN
ARG=PI*(XH(I)*ALPHA+YH(I)*BETA+ZH(I)*GAMMA)/WM
EV(I)=CMPLX(COS(-ARG),SIN(-ARG))
1 CONTINUE
RETURN
END

```

REVB

```

SUBROUTINE REVB(TH,PH,Y)
Y=0.0
IF(ABS(PH-45.0) .LT. (.1E-3)) Y=1.0
RETURN
END

```

Copy available to DDC does not
 permit fully legible reproduction

PINT

```

SUBROUTINE PINT(HHZ,HVT,LOWH,LIMH,LOWV,LIMV,MANYH,XH,YH,ZH,I,J,
INDEX,W,IDR,TDI)
DIMENSION XH(1),YH(1),ZH(1)
DATA PI,DEG/3.1415926535,0.01745329/
TDI=0.0
1210 IF(MANYH .LE. 0) GO TO 1200
FIHOZ=HHZ*DEG
FIVT=HVT*DEG
HLOW=FLOAT(LOWH)
VLOW=FLOAT(LOWV)
DINDEX=0.0
IIND=+1
DO 1000 JO=0,LIMH
DI=0.0
TH=FLOAT(JO)*HHZ+HLOW
JIND=+1
DO 1001 KO=0,LIMV
PH=FLOAT(KO)*HVT+VLOW
CALL FN(TH,PH,XH,YH,ZH,I,J,INDEX,W,IDR,X)
IF(KO .NE. 0) GO TO 1002
1003 DI=DI+X
GO TO 1001
1002 IF(KO .EQ. LIMV) GO TO 1003
DI=DI+X+X
IF(JIND .GT. 0) DI=DI+X+X
JIND=-JIND
1001 CONTINUE
IF(JO .NE. 0) GO TO 1005
1004 DINDEX=DINDEX+FIVT*DI/3.
GO TO 1000
1005 IF(JO .EQ. LIMH) GO TO 1004
DINDEX=DINDEX+2.*FIVT*DI/3.
IF(IIND .GT. 0) DINDEX=DINDEX+2.*FIVT*DI/3.
IIND=-IIND
1000 CONTINUE
TDI=TDI+FIHOZ*DINDEX/3.0
MANYH=MANYH-1
GO TO 1210
1200 CONTINUE
A=FLOAT(LOWV)*DEG
B=A+(FLOAT(LIMV)*HVT)*DEG
TDI=TDI/(2.*PI*(SIN(B)-SIN(A)))
RETURN
END

```

Copy available to DDC does not
 permit fully legible reproduction.

**COPY AVAILABLE TO DDC DOES NOT
 PERMIT FULLY LEGIBLE PRODUCTION**

FN

```

SUBROUTINE FN(THETA,PHI,XH,YH,ZH,I,J,IN,W,IDR,X)
DIMENSION XH(1),YH(1),ZH(1)
DATA PI,DEG/6.283185307,0.1745329E-01/
TH=THETA*DEG
PH=PHI*DEG
ALPHA=COS(PH)*SIN(TH)
BETA=COS(PH)*COS(TH)
GAMMA=-SIN(PH)
ARC=PI*((XH(1)-XH(J))*ALPHA+(YH(1)-YH(J))*BETA+(ZH(1)-ZH(J))*GAMMA/
5)/W
IF(IN.EQ.0) X=COS(ARC)*COS(PH)
IF(IN.EQ.1) X=SIN(ARC)*COS(PH)
IF(IDR.EQ.0) RETURN
CALL REVS(THETA,PHI,Y)
X=X*Y
RETURN
END

```

Copy available to DDC does not
 permit fully legible reproduction.

**COPY AVAILABLE TO DDC DOES NOT
 PERMIT FULLY LEGIBLE PRODUCTION**

A-9/A-10
 REVERSE BLANK

REFERENCES

1. A.I. Uzkov, "An Approach to the Problem of Optimum Directive Antennae Design," Comptes Rendus (Doklady) de l'Academie des Sciences de l'URSS 53, 1946, pp. 35-38.
2. C.T. Tai, "The Optimum Directivity of Uniformly Spaced Broadside Array of Dipoles," IEEE Trans. Antennas and Propagation, vol. AP-12, no. 4, 1964, pp. 447-454.
3. J.K. Butler, and H. Unz, "Beam Efficiency and Gain Optimization of Antenna Arrays with Nonuniform Spacings," Radio Science, vol. 2 (new series), no. 7, 1967, pp. 711-720.
4. M.T. Ma, Theory and Application of Antenna Arrays, John Wiley & Sons, New York, 1974.
5. D.K. Cheng, and F.I. Tseng, "Gain Optimization for Arbitrary Antenna Arrays," IEEE Trans. Antennas and Propagation, vol. AP-13, no. 6, 1965, pp. 973-974.
6. D.K. Cheng, and F.I. Tseng, "Maximization of Directive Gain for Circular and Elliptical Arrays," Proc. IEEE, vol. 114, no. 5, 1967, pp. 589-594.
7. Y.T. Lo, S.W. Lee, and Q.H. Lee, "Optimization of Directivity and Signal-to-Noise Ratio of an Arbitrary Antenna Array," Proc. IEEE, vol. 54, no. 8, 1966, pp. 1033-1045.
8. E.N. Gilbert, and S.P. Morgan, "Optimum Design of Directive Antenna Array Subject to Random Variations," Bell System Tech. J. 34, 1955, pp. 637-663.
9. H. Mermoz, "Filtrage Adapté et Utilization Optimale d'une Antennae," Proc. NATO Advanced Study Institute on Signal Processing with Emphasis on Underwater Acoustics, Grenoble, France, 1964.
10. A. Block, R.G. Medhurst, and S.D. Pool, "A New Approach to the Design of Superdirective Aerial Arrays," Proc. IEEE (London), 100, part III, 1953, pp. 303-314.
11. H.J. Riblet, "Note on the Maximum Directivity of an Antenna," Proc. IRE, 35, 1948, pp. 620-623.

12. L.J. Chu, "Physical Limitations of Omni-Directional Antennas," Journal of Applied Physics, 19, 1948, pp. 1163-1175.
13. N. Yaru, "A Note on Super-Gain Antenna Arrays," Proc. IRE, 39, 1951, pp. 1081-1084.
14. R.M. Wilmotte, "Note on Practical Limitations in the Directivity Antennas," Proc. IRE, 36, 1947, p. 878.
15. R.L. Pritchard, "Maximum Directivity Index of a Linear Point Array," JASA, vol. 26, no. 6, 1954, pp. 1034-1039.
16. R.L. Pritchard, "Optimum Directivity Patterns for Linear Point Arrays," JASA, vol. 25, no. 5, 1953, pp. 879-891.
17. J.J. Faran, and R. Hills, Jr., "Wide-Band Directivity of Receiving Arrays," Acoustical Research Lab Tech Memo No. 31, 1953.
18. D. Edelblute, J.M. Fisk, and G. Kinnison, "Criteria for Optimum-Signal-Detection Theory for Arrays," JASA, vol. 41, no. 1, 1967, pp. 199-205.
19. H. Cox, "Sensitivity Considerations in Adaptive Beamforming," in Signal Processing, Academic Press, London and New York, 1973, pp. 619-645.
20. F. Bryn, "Optimum Signal Processing of Three-Dimensional Arrays Operating on Gaussian Signals and Noises," JASA, vol. 34, (3), 1962, pp. 289-297.
21. A.H. Nuttall and D.W. Hyde, "A Unified Approach to Optimum and Suboptimum Processing for Arrays," NUSC Report #992, 1969.
22. N.L. Owsley, "A Recent Trend in Adaptive Spatial Processing for Sensor Arrays: Constrained Adaptation," in Signal Processing. Proceedings of NATO Advanced Study 1 Institute on Signal Processing. Academic Press, London and New York, 1973.
23. J.B. Lewis, and P.M. Schulttheiss, "Optimum and Conventional Detection Using Linear Array," JASA, vol. 49, (4), 1971, pp. 1083-1091.
24. F.R. Gantmacher, "The Theory of Matrices," Chelsea Publishing Co., New York, 1959.
25. D. Lee, and G.A. Leibiger, Computation of Beam Patterns and Directivity Indices for Three-Dimensional Arrays with Arbitrary Element Spacings, NUSC Technical Report 4687, 1974.

26. R.J. Urick, Principles of Underwater Sound for Engineers, McGraw-Hill Book Co., Inc., New York, 1967.
27. S. Zohar, "Toeplitz Matrix Inversion: The Algorithm of W.F. Trench," Journal of the ACM, vol. 16, no. 4, 1969, pp. 592-601.

TR 5375

INITIAL DISTRIBUTION LIST

Addressee	No. of Copies
ASN (R&D)	1
ONR, Code 102-OS, 412-3, 480, 485, 410	5
CNO, Code OP-095, -098, -96	3
CNM, Code MAT-03, -0302, SP-20	3
NAVSHIPRANDCEN, ANNA	1
NAVSHIPRANDCEN, CARD	1
NRL, Underwater Sound Reference Division	1
NAVOCEANO, Code 02, 7200	2
NAVSEASYSKOMHQ, SEA-032, -06H1, -06H1-1, -06H1-2, -06H1-3, -06H1-4, -09G3 (4), -660C, -660F, -661C	13
DTNSRDC	1
NAVUSEACEN	1
NUC, Pasadena (R. Vachon)	1
NAVPGSCOL	1
APL/UW, SEATTLE	1
ARL/PENN STATE, STATE COLLEGE (Prof. G. L. Wilson)	1
DDC, ALEXANDRIA	12
MARINE PHYSICAL LAB, Scripps	1
Lombard Systems, Inc. (Dr. Robert Baron), Mountain View, CA 94040	1